# EFFECT OF NONMAGNETIC PbO NANOPARTICLES ADDITION ON THE MICROSTRUCTURE AND ELECTRICAL TRANSPORT PROPERTIES OF YBa$_2$Cu$_3$O$_7$

## STEPHANIE KEONG WEI SAN

## UNIVERSITI MALAYSIA PAHANG

# UNIVERSITI MALAYSIA PAHANG

DECLARATION OF THESIS AND COPYRIGHT

Author's full name  :  Stephanie Keong Wei San

Date of birth        :  3 January 1993

Title               :  Effect of Nonmagnetic PbO Nanoparticles Addition on the

Microstructure and Electrical Transport Properties of

$YBa_2Cu_3O_7$

Academic Session    :  Semester I 2016/2017

I declare that this thesis is classified as:

|  | **CONFIDENTIAL** | (Contains confidential information under the Official Secret Act 1972) |
|---|---|---|
|  | **RESTRICTED** | (Contains restricted information as specified by the organization where research was done) |
| ■ | **OPEN ACCESS** | I agree that my thesis to be published as online open access (Full text) |

I acknowledge that Universiti Malaysia Pahang reserve the right as follows:

1.   The Thesis is the Property of Universiti Malaysia Pahang
2.   The Library of Universiti Malaysia Pahang has the right to make copies for the purpose of research only.
3.   The Library has the right to make copies of the thesis for academic exchange.

   Certified By:


_____               _____
   (Student's Signature)                              (Supervisor's Signature)

Stephanie Keong Wei San                      Dr. Muhammad Hafiz Bin Mazwir
930103-07-5218
Date:                                        Date:

EFFECT OF NONMAGNETIC PbO NANOPARTICLES
ADDITION ON THE MICROSTRUCTURE AND
ELECTRICAL TRANSPORT PROPERTIES OF
$YBa_2Cu_3O_7$

STEPHANIE KEONG WEI SAN

Thesis submitted in fulfillment of the requirements
for the award of the degree of
Bachelor of Applied Science (Honor) Material Technology

Faculty of Industrial Sciences & Technology
UNIVERSITI MALAYSIA PAHANG

DECEMBER 2016

## SUPERVISORS' DECLARATION

I hereby declare that I have checked the thesis and in my opinion, this thesis is adequate in terms of scope and quality for the award of the degree of Bachelor of Applied Science (Honor) Material Technology.

Signature

Name of Supervisor : DR. MUHAMMAD HAFIZ BIN MAZWIR

Position : SENIOR LECTURER

Date :

## STUDENT'S DECLARATION

I hereby declare that the work in this thesis is my own except for quotations and summaries which have been duly acknowledged. The thesis has not been accepted for any degree and is not concurrently submitted for award of other degree.

Signature     :

Name          :     STEPHANIE KEONG WEI SAN

ID Number     :     SC13050

Date          :

# DEDICATION

This thesis is dedicated to my beloved parents and esteemed lecturers

# ACKNOWLEDGEMENTS

As this thesis signifies the culmination of my four years of education in Material Technology, I would like to take this opportunity to express my sincere gratitude and appreciation to those who have supported and guided me throughout my undergraduate life.

First and foremost a huge acknowledgement of appreciation to my supervisor, Dr. Hafiz for his guidance, patience and continuous support towards the completion of this research. I could not asked for a better advisor and mentor for my research. Besides my supervisor, I would also like to express my gratitude towards my esteemed lecturers who were willing to impart their immense knowledge tirelessly throughout my entire undergraduate study.

Next, my sincere thanks also goes out to my fellow material technology lab mates and members for their stimulating discussion, for their assistance not only during lab but in classes as well and for their encouragement. Their continuous support and encouragement has enable me to enjoy my time here in university.

Last but not least, my greatest gratitude is dedicated to my parents for their love, support and sacrifice throughout my life. They are the backbone and structure of my life and the reason for my success. I would not be where I am today without them.

.

# ABSTRACT

Superconductors are materials that show zero resistance when subjected to temperature under its critical temperature. Yttrium Barium Copper Oxide (YBCO) was prepared using solid state reaction method by grinding, sintering and finally pressing the samples into pellets. The objective of the research ws to study the change in (i) microstructure and (ii) electrical transport properties of YBCO with the addition of 0.00 wt%, 0.01 wt%, 0.02 wt%, 0.03 wt% and 0.04 wt% nonmagnetic PbO nanoparticles, as well as to develop a laboratory scale method in determining the electrical properties of YBCO at liquid nitrogen temperature. The presence of superconductivity was tested and confirmed when the samples was allowed to levitate above a row of Neodymium magnet and the sample with 0.04 wt% PbO nanoparticle showed the longest levitation time. From the results obtained from the X-ray diffraction, it was noted that there was minimal changes to the microstructure and composition of the superconductor when the PbO nanoparticle was added to them. A four point probe was developed to test the critical temperature of the YBCO superconductor. The results obtained does not fulfil the expected results as the critical temperature obtained for the added sample is lower than that of the referenced results which is 90 K.

# ABSTRAK

Superkonduktor adalah bahan-bahan yang menunjukkan rintangan sifar apabila diletakkan suhu di bawah suhu kritikal. Yttrium Barium Copper Oxide (YBCO) telah disediakan dengan menggunakan kaedah tindak balas keadaan pepejal dengan mengisar, menyintar dan akhirnya menekan sampel ke dalam pelet. Objektif penyelidikan adalah untuk mengkaji perubahan dalam (i) mikrostruktur dan (ii) ciri-ciro elektrik YBCO dengan tambahan 0.00 wt%, 0.01 wt%, 0.02 wt%, 0.03 wt% dan 0.04 wt% nanozarah PbO , serta untuk mewujudkan kaedah skala makmal untuk menentukan ciri-ciri elektrik YBCO pada suhu nitrogen cecair. Kehadiran kesuperkonduksian telah diuji dan disahkan apabila sampel dibiarkan terapung di atas deretan magnet Neodymium dan sampel dengan 0.04 wt% PbO nanozarah menunjukkan masa pengangkatan paling lama. Daripada keputusan yang diperolehi daripada pembelauan sinar-X, didapati bahawa terdapat perubahan yang minimum kepada mikrostruktur dan komposisi superkonduktor apabila nanozarah PbO telah ditamba. Penduga empat titik telah diwujudkan untuk menguji suhu kritikal superkonduktor YBCO. Keputusan yang diperolehi tidak memenuhi hasil yang diharapkan kerana suhu kritikal yang diperolehi bagi sampel yang telah ditambah dengan nanozarah adalah lebih rendah daripada keputusan yang dirujuk iaitu 90 K.

# TABLE OF CONTENTS

# LIST OF TABLES

# LIST OF FIGURES

# LIST OF SYMBOLS

| | | |
|---|---|---|
| ~ | - | approximately |
| wt. % | - | weight percent |
| % | - | percent |
| $2\theta$ | - | Bragg angle |
| $^{o}C$ | - | degree celcius |
| K | - | Kelvin |
| Å | - | angstrom ($10^{-10}$) |
| g | - | grams |
| $t$ | - | time |
| $\Omega$ | - | Ohm |
| V | - | voltage |
| I | - | current |
| $T_c$ | - | critical temperature |
| $J_c$ | - | critical current density |
| $H_c$ | - | critical magnetic field |
| B | - | magnetic flux |
| $\Xi$ | - | coherence length |
| $\Lambda$ | - | penetration depth |

# LIST OF ABBREVIATIONS

| | | |
|---|---|---|
| $PbO$ | - | Lead Oxide |
| $Y_2O_3$ | - | Yttrium Oxide |
| $BaCo_3$ | - | Barium Carbonate |
| $CuO$ | - | Copper Oxide |
| Y123 | - | Yttrium Barium Copper Oxide |
| YBCO | - | Yttrium Barium Copper Oxide |
| XRD | - | X-Ray Diffraction |
| SEM | - | Scanning Electron Microscopy |
| BCS | - | Bardeen Cooper Schrieffer |
| GL | - | Ginzburg-Landau |
| $Al$ | - | Aluminium |

# CHAPTER 1

# INTRODUCTION

## 1.1    Background Of The Proposed Study

Superconductivity is a unique phenomenon that occurs when a material below a transition temperature or critical temperature shows zero resistance. Superconductivity was discovered in 1911 by H.K. Onnes when he observed that as mercury is cooled to the temperature of liquid helium (4.0 K), its resistance vanishes abruptly. Subsequent research and studies follows the discoveries of other superconductor such as lead, aluminium and tin.
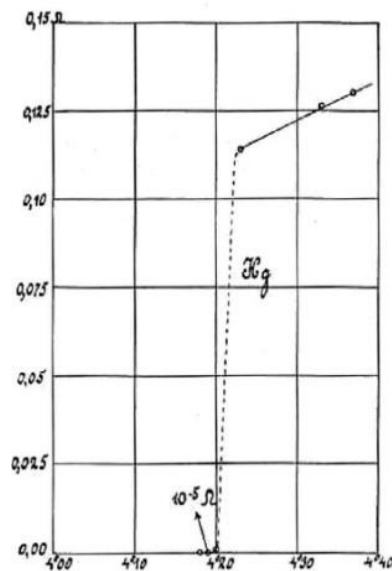


*Figure 1. 1.*    Electrical resistance of mercury against temperature

Source: Reproduced from (Onnes K., 1911)

In 1986, a brittle ceramic compound was discovered to superconduct at 30 K; the highest temperature known at the time by Alex Muller and Georg Bednorz. This discovery of high temperature superconductivity lead to a worldwide research on ceramics that are able to superconduct and in January of 1987, a group of researchers at the University of Alabama-Huntsville discovered YBCO, a material that is able to superconduct at a temperature greater than liquid nitrogen. (Wu et al., 1987). The expulsion of magnetic field by a superconductor, also known as Meissner effect was discovered in 1933 by two German researchers, Walther Meissner and Robert Ochsenfeld. This principle of Meissner effect explains perfect diamagnetism; the ability to completely repel a magnetic field in superconductors.
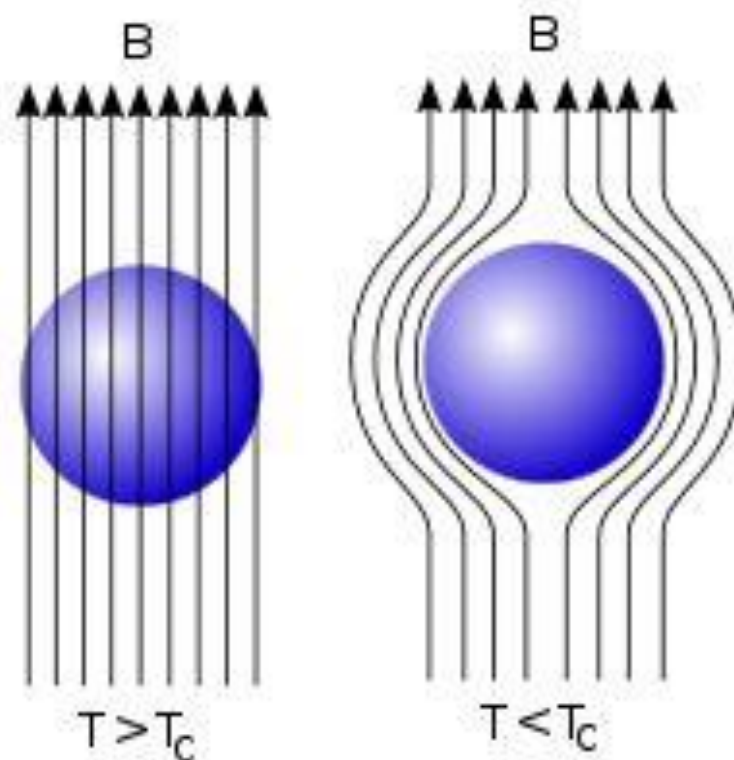


*Figure 1. 2.*     Meissner effect showing magnetic repulsion in superconductor below critical temperature

Source: Reproduced from (Kittel C., 2005)

The theory of superconductivity explains the occurrence of zero resistance in low temperature superconductor. BCS theory or Bardeen-Cooper-Schrieffer theory, coined after the scientists who discovered it, infer that electrons are coupled into Cooper pairs formed through the interaction with the crystal lattice resulting from a slight attraction between the electrons in relation to lattice vibration or phonons. (Bardeen et al.,1957). However, since the publication of BCS theory in the letter "Microscopic Theory of Superconductivity" in 1957, it is believed that the theory alone does not effectively explain the presence of superconductivity in high temperature superconductors. This is due to the its failure to show strong electron-lattice interaction as required in high temperature superconductor. (Miller et al., 2012)

While the microscopic theory of superconductivity can be explained by BCS theory, the macroscopic theory can be postulated by Ginzburg-Landau (GL) theory. The theory involves two characteristics; the coherence length, $\xi$ and the penetration depth, $\lambda$. The GL parameter, $\kappa$ is therefore the ratio of $\lambda$ to $\xi$ and has a limiting factor of $\kappa = 1/\sqrt{2}$, which separates the superconductors with positive surface energy where $\kappa < 1/\sqrt{2}$ from the negative surface energy where $\kappa > 1/\sqrt{2}$. (Suzuki, M et al., 2007)

Superconductors can therefore be sorted into two types, mainly type I superconductor and type II superconductor based on the materials behaviour on its transition from superconducting state to normal state. (Abd-Shukor, R., 2004). For type 1 superconductor, when the applied magnetic field is greater than its critical field, $B_c$ the material becomes non-superconducting or normal where its resistance is non-zero. There is no field penetration provided the applied field is less than its critical field, $B_c$. Type 1 superconductor behaves in accordance to the microscopic mechanism as describe by the BCS theory.
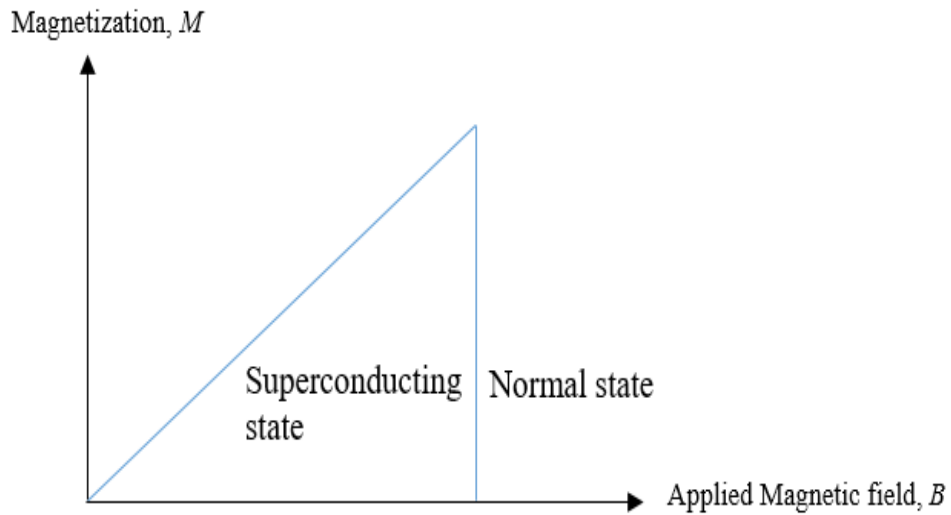
*Figure 1. 3.*     Magnetization of type I superconductors depending on the applied field.

On the other hand, in type-II superconductor the transition from superconducting to normal state is not immediate but gradual. When the applied field is bounded by the lower critical field and the upper critical field, type II superconductor demonstrates the occurrence of partial penetration of magnetic field in the form of fine filaments or vortex. (Abrikosov, A., 2003). The superconductor is said to be in a mixed state. Below the lower critical field, the superconductor behaves like type I superconductor while above the upper critical field the material is in the normal state.
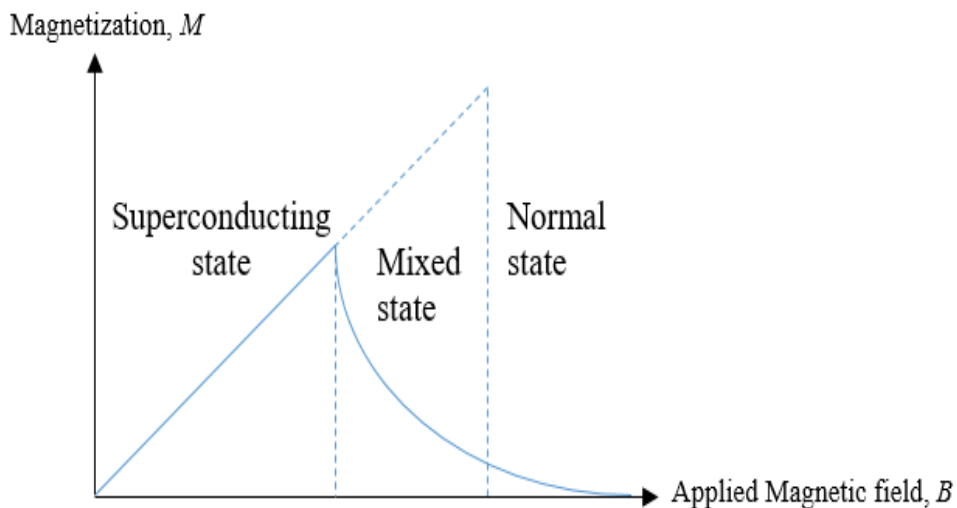


*Figure 1. 4.*     Magnetization of type II superconductors depending on the applied field.

Since the discovery its discovery in 1911, superconductor has been utilized in a variety of application. One of the most notable application is in transport vehicles where superconductors function exceptionally well in response to magnetic levitation. With the use of superconducting magnets located intermittently along the tracks, a magnetic field is created enabling both levitation and propulsion of the MAGLEV. April 3, 1997 marks the historic opening of Yamanashi Maglev Test Line, a landmark for the commercial use of MAGLEV technology. However, despite its advancement, MAGLEV vehicles are limited by several factors such as temperature requirements and political as well as environmental concerns.

Another example where superconductor is proven to be practically more superior to other materials is in Magnetic Resonance Imaging (MRI), an application that is still widely used in the medical field. MRI works by aligning the hydrogen nuclei from a human body with the strong superconductor-derived magnetic field. Since protons at different areas realign at different frequency, its magnetic resonance can be utilized to map out soft tissue of the human body.

## 1.2    Problem Statement

Despite its outstanding potential to be the leading material in the advancement technology, superconductor its development is constraint by multiple factors. One of the major limitation is their restricted range of operating temperatures. Type-II superconductor has an obvious advantage of Type-I superconductor as Type II is able to operate at a higher $T_c$ compared to Type-I. However, the highest $T_c$ recorded thus far is only 138 K, limiting their range of practical application in consumer electronics.

Besides the limitation related to the theoretical aspect of superconductor, there is also a restriction in terms of experimentation due to the lack of method and equipment in the laboratory to test the electronic properties reliably and precisely.

**1.3    Objectives Of Research**

Objectives of this research are:

i.    To study the change in the microstructure of YBCO with the addition of 0.00 wt%, 0.01 wt%, 0.02 wt%, 0.03 wt% and 0.04 wt% nonmagnetic PbO nanoparticles

ii.   To study the electrical transport properties of YBCO with the addition of 0.00 wt%, 0.01 wt%, 0.02 wt%, 0.03 wt% and 0.04 wt% nonmagnetic PbO nanoparticles.

iii.  To develop a laboratory scale method in determining the electrical properties of YBCO at liquid nitrogen temperature

**1.4    Scope Of Study**

The initial stages of the research involved the fabrication of the YBCO superconductor. This involves three processes which are hand grinding, sintering and pelletisation

After the fabrication process was the characterization of the YBCO superconductor. The critical temperature at liquid nitrogen temperature was characterized using four-point probe method. The microstructural changes were observed using XRD and SEM machine. The Meissner effect of the YBCO superconductor was also be observed.

Due to the lack of equipment in the laboratory, a fast, reliable and precise technique of determining the electrical transport properties of YBCO at liquid nitrogen temperature (77.2K) using four-point probe was developed.

**CHAPTER 2**

**LITERATURE REVIEW**

## 2.1    YBCO Introduction

In 1987, M. K. Wu and a team of researchers investigated the multiple-phase Y-Ba-Cu-O compound at ambient temperature. They were able to observe an unfluctuating and reproducible superconductivity transition between 80 and 93 K both resistively and magnetically. To achieve superconductivity above 77 K, lattice parameter, the valence ratio and the sample treatment play an important role. (Wu et al, 1987)
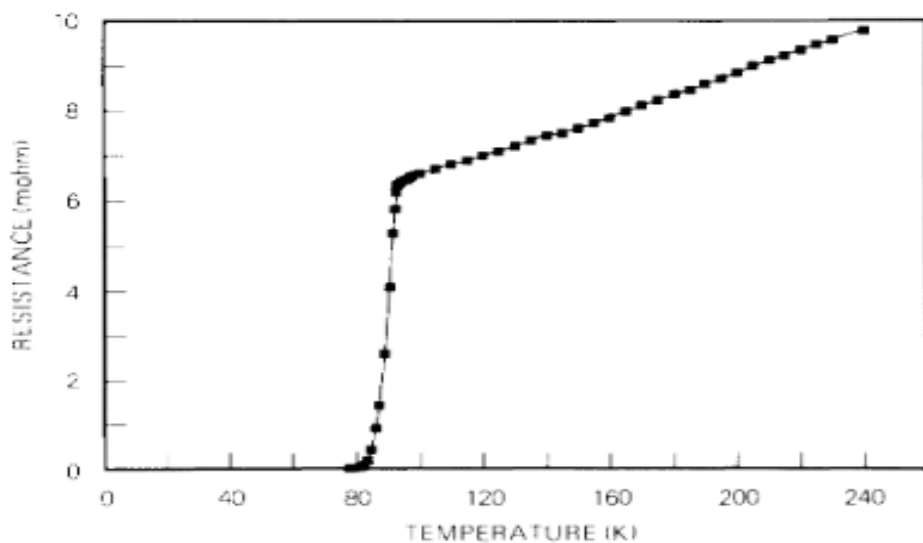


*Figure 2. 1.*    Magnetic effect on resistance in YBCO

Source: Reproduced from (Wu et al., 1987)

## 2.2    Structure Of YBCO

A clear grasp on the structure is a prerequisite for understanding the properties of a superconducting material. Therefore, the basic structure of YBCO superconductor has been determined as a distorted, oxygen deficient multi-layered perovskite structure. Specific points of the structure especially the configuration of Cu-O contributes to the superconducting mechanism of the material. The perovskite structure of YBCO consist of one yttrium atom for every third barium atom resulting in the $YBa_2Cu_3O_{7-\delta}$ formula. The crystal structure of YBCO shows that there are oxygen vacancies in a Cu layer and the critical temperature of the superconducting material is dependent on the oxygen content. Hence, superconductivity takes place in between the layers of $CuO_2$. The critical temperature of the superconducting material increases with the increase in the layers of $CuO_2$. (G. Alecu, 2004)
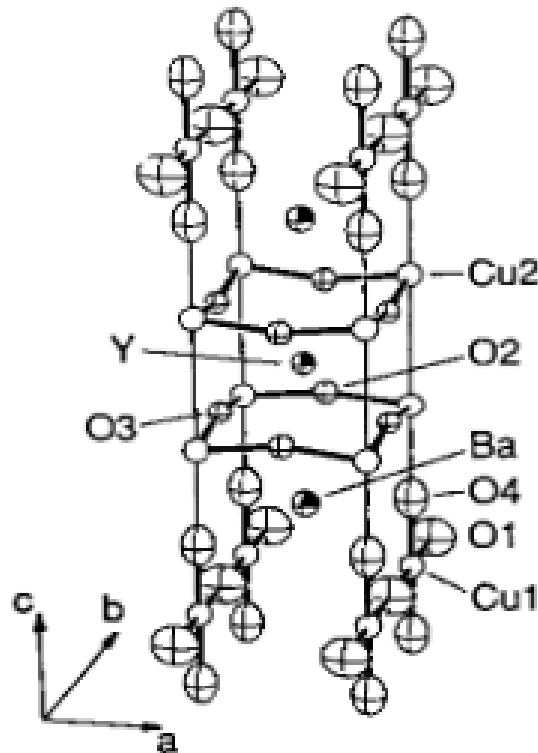


*Figure 2. 2.*    Structure of the double layered YBCO compound

Source: Reproduced from (Alecu, 2004)

8

## 2.3    Effects Of The Addition Of Nanoparticles

Over the years, numerous research has been conducted to achieve an improved and more efficient superconducting materials by addition of nanoparticles. R. Abd-Shukor et al., (2014) reported that with the addition of nano-sized $Co_3O_4$, there was no significant changes to the onset transition temperature, $T_c$ for low $Co_3O_4$ ($x \geq 0.02$ wt%). However, with the increase in $Co_3O_4$ content, the $T_c$ decreases monotonically suggesting the breaking of pairs for $x = 0.03$ to $x = 0.12$ wt%. A widening of the superconducting transition width was also examined with increasing $Co_3O_4$ content and a swift enhanced broadening was observed for $x \geq 0.11$ wt%. In addition to that, a homogenous distribution of $Co_3O_4$ throughout the sample was observed under scanning electron micrographs.
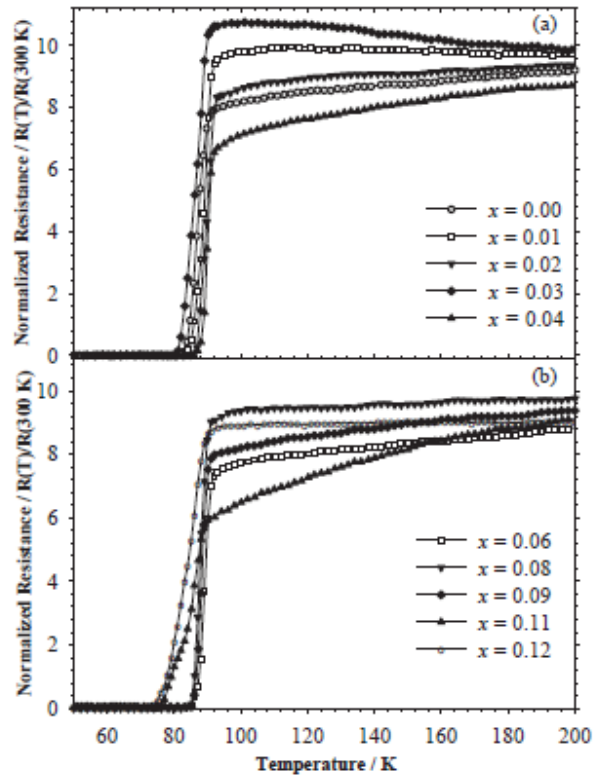


*Figure 2. 3.*    Electrical resistance versus temperature curves of YBa2CuO7-δ for (a) $x = 0$ to $0.04$ and (b) $x = 0$ to $0.12$

Source: Abd-Shukor et al. (2014)

In another research by S.N. Abd Ghani et al., (2012), the effects of $Fe_3O_4$ nanoparticles addition on the superconducting and transport properties of $YBa_2Cu_3O_{7-\delta}$ was examined. From the study, it was discovered that the sample containing 0.02 wt% $Fe_3O_4$ has the highest $T_c$ at 87 K and the highest $J_c$ at 77K up to 1683 mA/cm$^2$. However, with excessive addition of $Fe_3O_4$ (> 0.02 wt%), the $T_c$ and $J_c$ was suppressed. Hence, based on the results, it was concluded that $Fe_3O_4$ is able to act as an effective flux pinning centers and optimized $J_c$. Small amounts of magnetic nanoparticles can be applied to enhance the transport critical density of YBCO superconductor.
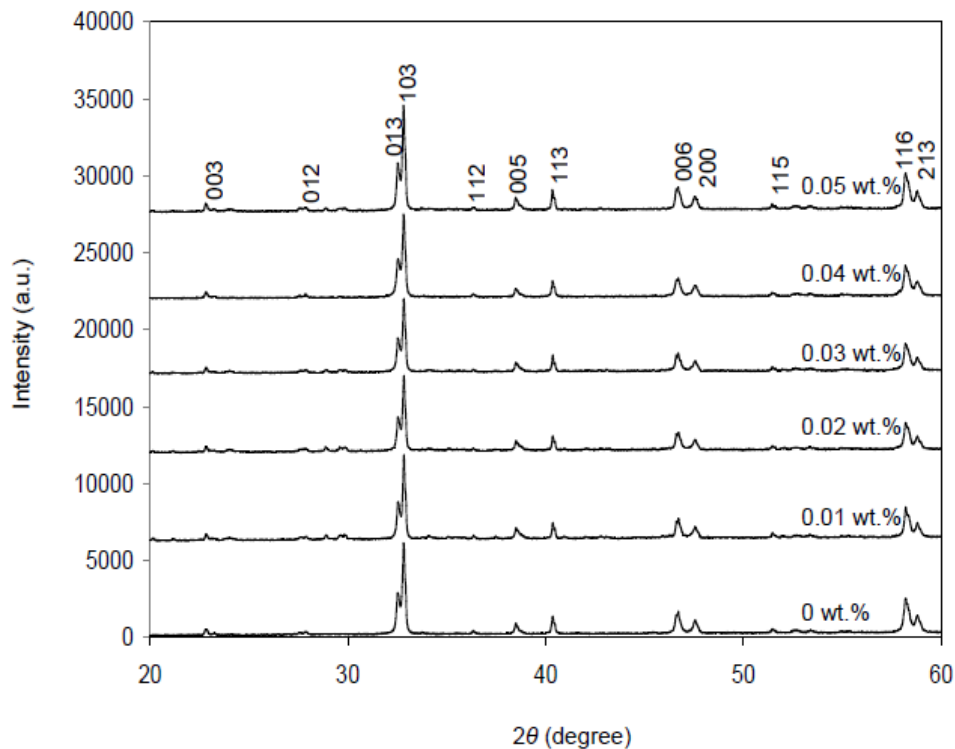


*Figure 2. 4.*     X-ray diffraction patterns of YBCO with the addition of different amount of $Fe_3O_4$

Source: Reproduced from (Nabil A. A. Yahya et at., 2013)

In regards to the addition of PbO nanoparticles, a research by Nabil A. A. Yahya and Abd-Shukor was conducted in 2013 to observe the effects of PbO addition to electrical transport properties of $(Bi_{1.6}Pb_{0.4})Sr_2Ca_2Cu_3O_{10}$. Due to certain limiting factors, such as its grain alignment, weak links between the grains and weak pinning of flux lines, the critical current density of $(Bi_{1.6}Pb_{0.4})Sr_2Ca_2Cu_3O_{10}$ decreases in relation with the

increase of the magnetic field and temperature. In the research, (Bi, Pb)-2223(PbO)$_x$ superconductor was fabricated using acetate co-precipitate method. There was a significant enhancement to the $J_c$ with the addition of nanosized PbO with the highest recorded $J_c$ for $x = 0.05$ wt%. The improvement of critical current density is believed to be due to the effective artificial pinning centres providing additional flux pinning centers in the $(Bi_{1.6}Pb_{0.4})Sr_2Ca_2Cu_3O_{10}$.
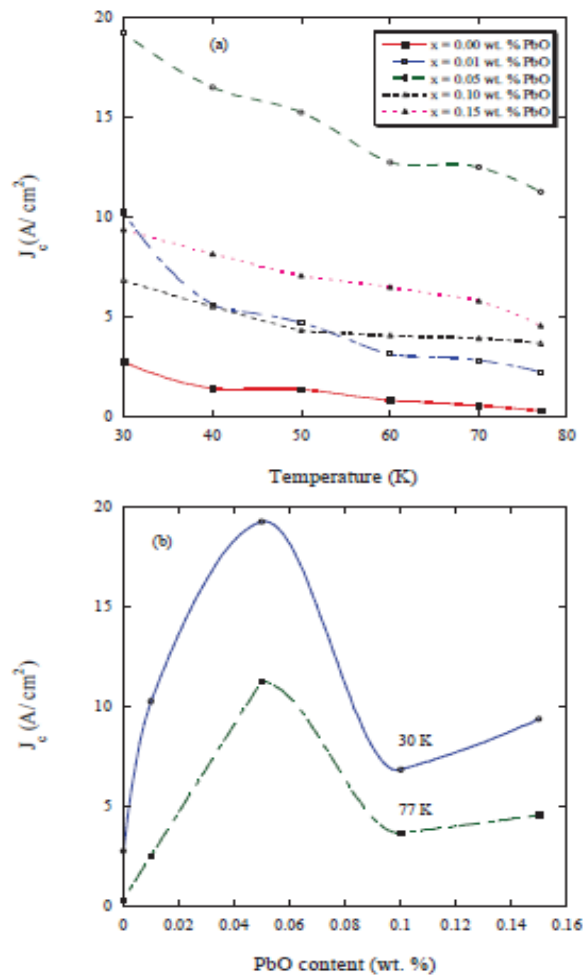


*Figure 2. 5.* *Jc* of (Bi, Pb)-2223(PbO)x; (a) as a function of the temperature (30-77 K), and (b) PbO content at 30 and 77 K.

Source: Reproduced from (Nabil A. A. Yahya et al., 2013)

## 2.4 Four-Point Probe

The four-point probe was first employed by L B. Valdes in 1954 when he tested the resistivity measurements on germanium. The method involves four probes placed in direct contact with the surface of the material. Current is then allowed to flow through the two probes at the far end and the potential is measured using a voltmeter across the inner pair of probes. When employing the method, it is assumed that the resistivity is uniform across the material in the area of measurement, the four probes are lying in a straight line on the surface of the material and the surface is flat, void of surface leakage. (L. B. Valdes, 1954)



*Figure 2. 6.* Model of the four probe resistivity measurements

Source: Reproduced from (L. B. Valdes, 1954)



*Figure 2. 7.* Circuit used for resistivity measurements

Source: Reproduced from (L. B. Valdes, 1954)

12

Along with the four-point probe, a thermocouple was utilized in measuring and controlling the temperature at which the sample is placed in. In this research, type T thermocouple was chosen due to its temperature range of -270°C to 370°C which will be able to measure the temperature of the liquid nitrogen. Type T is also known as copper-constantan thermocouple due to the material from which it is made. A simple formula can be employed for the calculation of junction temperature from the measured EMF. Table 1.1 is the thermocouple reference table which shows the thermoelectric voltage as a function of temperature (°C)

Table 2. 1.
*Type T thermocouple reference table*

Thermoelectric Voltage in Millivolts

| °C | -10 | -9 | -8 | -7 | -6 | -5 | -4 | -3 | -2 | -1 | 0 | °C |
|---|---|---|---|---|---|---|---|---|---|---|---|---|
| -260 | -6.258 | -6.256 | -6.255 | -6.253 | -6.251 | -6.248 | -6.245 | -6.242 | -6.239 | -6.236 | -6.232 | -260 |
| -250 | -6.232 | -6.228 | -6.223 | -6.219 | -6.214 | -6.209 | -6.204 | -6.198 | -6.193 | -6.187 | -6.180 | -250 |
| -240 | -6.180 | -6.174 | -6.167 | -6.160 | -6.153 | -6.146 | -6.138 | -6.130 | -6.122 | -6.114 | -6.105 | -240 |
| -230 | -6.105 | -6.096 | -6.087 | -6.078 | -6.068 | -6.059 | -6.049 | -6.038 | -6.028 | -6.017 | -6.007 | -230 |
| -220 | -6.007 | -5.996 | -5.985 | -5.973 | -5.962 | -5.950 | -5.938 | -5.926 | -5.914 | -5.901 | -5.888 | -220 |
| -210 | -5.888 | -5.876 | -5.863 | -5.850 | -5.836 | -5.823 | -5.809 | -5.795 | -5.782 | -5.767 | -5.753 | -210 |
| -200 | -5.753 | -5.739 | -5.724 | -5.710 | -5.695 | -5.680 | -5.665 | -5.650 | -5.634 | -5.619 | -5.603 | -200 |
| -190 | -5.603 | -5.587 | -5.571 | -5.555 | -5.539 | -5.523 | -5.506 | -5.489 | -5.473 | -5.456 | -5.439 | -190 |
| -180 | -5.439 | -5.421 | -5.404 | -5.387 | -5.369 | -5.351 | -5.334 | -5.316 | -5.297 | -5.279 | -5.261 | -180 |
| -170 | -5.261 | -5.242 | -5.224 | -5.205 | -5.186 | -5.167 | -5.148 | -5.128 | -5.109 | -5.089 | -5.070 | -170 |
| -160 | -5.070 | -5.050 | -5.030 | -5.010 | -4.989 | -4.969 | -4.949 | -4.928 | -4.907 | -4.886 | -4.865 | -160 |
| -150 | -4.865 | -4.844 | -4.823 | -4.802 | -4.780 | -4.759 | -4.737 | -4.715 | -4.693 | -4.671 | -4.648 | -150 |
| -140 | -4.648 | -4.626 | -4.604 | -4.581 | -4.558 | -4.535 | -4.512 | -4.489 | -4.466 | -4.443 | -4.419 | -140 |
| -130 | -4.419 | -4.395 | -4.372 | -4.348 | -4.324 | -4.300 | -4.275 | -4.251 | -4.226 | -4.202 | -4.177 | -130 |
| -120 | -4.177 | -4.152 | -4.127 | -4.102 | -4.077 | -4.052 | -4.026 | -4.000 | -3.975 | -3.949 | -3.923 | -120 |
| -110 | -3.923 | -3.897 | -3.871 | -3.844 | -3.818 | -3.791 | -3.765 | -3.738 | -3.711 | -3.684 | -3.657 | -110 |
| -100 | -3.657 | -3.629 | -3.602 | -3.574 | -3.547 | -3.519 | -3.491 | -3.463 | -3.435 | -3.407 | -3.379 | -100 |
| -90 | -3.379 | -3.350 | -3.322 | -3.293 | -3.264 | -3.235 | -3.206 | -3.177 | -3.148 | -3.118 | -3.089 | -90 |
| -80 | -3.089 | -3.059 | -3.030 | -3.000 | -2.970 | -2.940 | -2.910 | -2.879 | -2.849 | -2.818 | -2.788 | -80 |
| -70 | -2.788 | -2.757 | -2.726 | -2.695 | -2.664 | -2.633 | -2.602 | -2.571 | -2.539 | -2.507 | -2.476 | -70 |
| -60 | -2.476 | -2.444 | -2.412 | -2.380 | -2.348 | -2.316 | -2.283 | -2.251 | -2.218 | -2.186 | -2.153 | -60 |
| -50 | -2.153 | -2.120 | -2.087 | -2.054 | -2.021 | -1.987 | -1.954 | -1.920 | -1.887 | -1.853 | -1.819 | -50 |
| -40 | -1.819 | -1.785 | -1.751 | -1.717 | -1.683 | -1.648 | -1.614 | -1.579 | -1.545 | -1.510 | -1.475 | -40 |
| -30 | -1.475 | -1.440 | -1.405 | -1.370 | -1.335 | -1.299 | -1.264 | -1.228 | -1.192 | -1.157 | -1.121 | -30 |
| -20 | -1.121 | -1.085 | -1.049 | -1.013 | -0.976 | -0.940 | -0.904 | -0.867 | -0.830 | -0.794 | -0.757 | -20 |
| -10 | -0.757 | -0.720 | -0.683 | -0.646 | -0.608 | -0.571 | -0.534 | -0.496 | -0.459 | -0.421 | -0.383 | -10 |
| 0 | -0.383 | -0.345 | -0.307 | -0.269 | -0.231 | -0.193 | -0.154 | -0.116 | -0.077 | -0.039 | 0.000 | 0 |

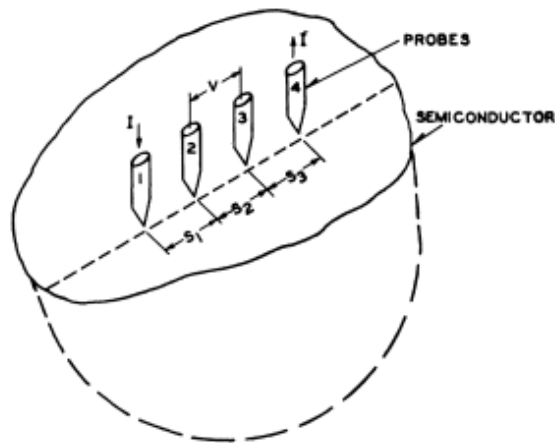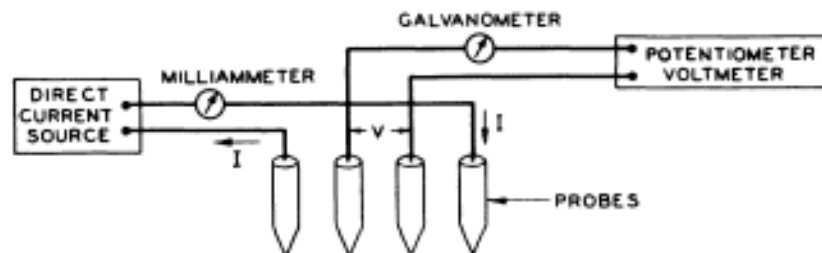| °C | 0 | 1 | 2 | 3 | 4 | 5 | 6 | 7 | 8 | 9 | 10 | °C |
|---|---|---|---|---|---|---|---|---|---|---|---|---|
| 0 | 0.000 | 0.039 | 0.078 | 0.117 | 0.156 | 0.195 | 0.234 | 0.273 | 0.312 | 0.352 | 0.391 | 0 |
| 10 | 0.391 | 0.431 | 0.470 | 0.510 | 0.549 | 0.589 | 0.629 | 0.669 | 0.709 | 0.749 | 0.790 | 10 |
| 20 | 0.790 | 0.830 | 0.870 | 0.911 | 0.951 | 0.992 | 1.033 | 1.074 | 1.114 | 1.155 | 1.196 | 20 |
| 30 | 1.196 | 1.238 | 1.279 | 1.320 | 1.362 | 1.403 | 1.445 | 1.486 | 1.528 | 1.570 | 1.612 | 30 |
| 40 | 1.612 | 1.654 | 1.696 | 1.738 | 1.780 | 1.823 | 1.865 | 1.908 | 1.950 | 1.993 | 2.036 | 40 |
| 50 | 2.036 | 2.079 | 2.122 | 2.165 | 2.208 | 2.251 | 2.294 | 2.338 | 2.381 | 2.425 | 2.468 | 50 |
| 60 | 2.468 | 2.512 | 2.556 | 2.600 | 2.643 | 2.687 | 2.732 | 2.776 | 2.820 | 2.864 | 2.909 | 60 |
| 70 | 2.909 | 2.953 | 2.998 | 3.043 | 3.087 | 3.132 | 3.177 | 3.222 | 3.267 | 3.312 | 3.358 | 70 |
| 80 | 3.358 | 3.403 | 3.448 | 3.494 | 3.539 | 3.585 | 3.631 | 3.677 | 3.722 | 3.768 | 3.814 | 80 |
| 90 | 3.814 | 3.860 | 3.907 | 3.953 | 3.999 | 4.046 | 4.092 | 4.138 | 4.185 | 4.232 | 4.279 | 90 |
| 100 | 4.279 | 4.325 | 4.372 | 4.419 | 4.466 | 4.513 | 4.561 | 4.608 | 4.655 | 4.702 | 4.750 | 100 |
| 110 | 4.750 | 4.798 | 4.845 | 4.893 | 4.941 | 4.988 | 5.036 | 5.084 | 5.132 | 5.180 | 5.228 | 110 |
| 120 | 5.228 | 5.277 | 5.325 | 5.373 | 5.422 | 5.470 | 5.519 | 5.567 | 5.616 | 5.665 | 5.714 | 120 |
| 130 | 5.714 | 5.763 | 5.812 | 5.861 | 5.910 | 5.959 | 6.008 | 6.057 | 6.107 | 6.156 | 6.206 | 130 |
| 140 | 6.206 | 6.255 | 6.305 | 6.355 | 6.404 | 6.454 | 6.504 | 6.554 | 6.604 | 6.654 | 6.704 | 140 |
| 150 | 6.704 | 6.754 | 6.805 | 6.855 | 6.905 | 6.956 | 7.006 | 7.057 | 7.107 | 7.158 | 7.209 | 150 |
| 160 | 7.209 | 7.260 | 7.310 | 7.361 | 7.412 | 7.463 | 7.515 | 7.566 | 7.617 | 7.668 | 7.720 | 160 |
| 170 | 7.720 | 7.771 | 7.823 | 7.874 | 7.926 | 7.977 | 8.029 | 8.081 | 8.133 | 8.185 | 8.237 | 170 |
| 180 | 8.237 | 8.289 | 8.341 | 8.393 | 8.445 | 8.497 | 8.550 | 8.602 | 8.654 | 8.707 | 8.759 | 180 |
| 190 | 8.759 | 8.812 | 8.865 | 8.917 | 8.970 | 9.023 | 9.076 | 9.129 | 9.182 | 9.235 | 9.288 | 190 |
| 200 | 9.288 | 9.341 | 9.395 | 9.448 | 9.501 | 9.555 | 9.608 | 9.662 | 9.715 | 9.769 | 9.822 | 200 |
| 210 | 9.822 | 9.876 | 9.930 | 9.984 | 10.038 | 10.092 | 10.146 | 10.200 | 10.254 | 10.308 | 10.362 | 210 |
| 220 | 10.362 | 10.417 | 10.471 | 10.525 | 10.580 | 10.634 | 10.689 | 10.743 | 10.798 | 10.853 | 10.907 | 220 |
| 230 | 10.907 | 10.962 | 11.017 | 11.072 | 11.127 | 11.182 | 11.237 | 11.292 | 11.347 | 11.403 | 11.458 | 230 |
| 240 | 11.458 | 11.513 | 11.569 | 11.624 | 11.680 | 11.735 | 11.791 | 11.846 | 11.902 | 11.958 | 12.013 | 240 |
| 250 | 12.013 | 12.069 | 12.125 | 12.181 | 12.237 | 12.293 | 12.349 | 12.405 | 12.461 | 12.518 | 12.574 | 250 |
| 260 | 12.574 | 12.630 | 12.687 | 12.743 | 12.799 | 12.856 | 12.912 | 12.969 | 13.026 | 13.082 | 13.139 | 260 |
| 270 | 13.139 | 13.196 | 13.253 | 13.310 | 13.366 | 13.423 | 13.480 | 13.537 | 13.595 | 13.652 | 13.709 | 270 |
| 280 | 13.709 | 13.766 | 13.823 | 13.881 | 13.938 | 13.995 | 14.053 | 14.110 | 14.168 | 14.226 | 14.283 | 280 |
| 290 | 14.283 | 14.341 | 14.399 | 14.456 | 14.514 | 14.572 | 14.630 | 14.688 | 14.746 | 14.804 | 14.862 | 290 |
| 300 | 14.862 | 14.920 | 14.978 | 15.036 | 15.095 | 15.153 | 15.211 | 15.270 | 15.328 | 15.386 | 15.445 | 300 |
| 310 | 15.445 | 15.503 | 15.562 | 15.621 | 15.679 | 15.738 | 15.797 | 15.856 | 15.914 | 15.973 | 16.032 | 310 |
| 320 | 16.032 | 16.091 | 16.150 | 16.209 | 16.268 | 16.327 | 16.387 | 16.446 | 16.505 | 16.564 | 16.624 | 320 |
| 330 | 16.624 | 16.683 | 16.742 | 16.802 | 16.861 | 16.921 | 16.980 | 17.040 | 17.100 | 17.159 | 17.219 | 330 |
| 340 | 17.219 | 17.279 | 17.339 | 17.399 | 17.458 | 17.518 | 17.578 | 17.638 | 17.698 | 17.759 | 17.819 | 340 |
| 350 | 17.819 | 17.879 | 17.939 | 17.999 | 18.060 | 18.120 | 18.180 | 18.241 | 18.301 | 18.362 | 18.422 | 350 |
| 360 | 18.422 | 18.483 | 18.543 | 18.604 | 18.665 | 18.725 | 18.786 | 18.847 | 18.908 | 18.969 | 19.030 | 360 |
| 370 | 19.030 | 19.091 | 19.152 | 19.213 | 19.274 | 19.335 | 19.396 | 19.457 | 19.518 | 19.579 | 19.641 | 370 |
| 380 | 19.641 | 19.702 | 19.763 | 19.825 | 19.886 | 19.947 | 20.009 | 20.070 | 20.132 | 20.193 | 20.255 | 380 |
| 390 | 20.255 | 20.317 | 20.378 | 20.440 | 20.502 | 20.563 | 20.625 | 20.687 | 20.748 | 20.810 | 20.872 | 390 |
| °C | 0 | 1 | 2 | 3 | 4 | 5 | 6 | 7 | 8 | 9 | 10 | °C |

13

# CHAPTER 3

# MATERIALS AND METHODS

## 3.1    Introduction

The YBa$_2$Cu$_3$O$_7$ superconductor powder in this study will be prepared by solid state reaction technique as is typically employed when preparing polycrystalline material. Cave et al., 2007 defines the process as a reaction between or within solid reactants to yield a solid product. After the weight of each raw material was calculated based on their balanced chemical equation, the process will use 4.52g yttrium oxide (Y$_2$O$_3$), 15.87 g barium carbonated (BaCO$_3$) and 9.9 g copper oxide (CuO). As in typical ceramic procedures, high purity of about 99.99% of Y$_2$O$_3$, BaCO$_3$, and CuO will be used as starting materials. These powders are to be grinded thoroughly and sintered in an oven at $900°C$ for 48 hours with intermittent grinding. Then, nonmagnetic PbO powder with varying amounts will be added to the YBCO powder. The mixed powders will then be grinded and pressed into pellets. After sintering the pellets at 900°C for 24 hours, they will be subjected to a number of process to characterize the YBCO superconductor.

The process of characterization includes determining the resistivity, critical current density, $J_c$ and critical temperature, $T_c$ of the superconductor using Four Point Probe method, determining the microstructure using scanning electron microscope (SEM) and determining the composition and phase of the YBCO using X-ray Diffractometer.

**3.2    Flow Chart**
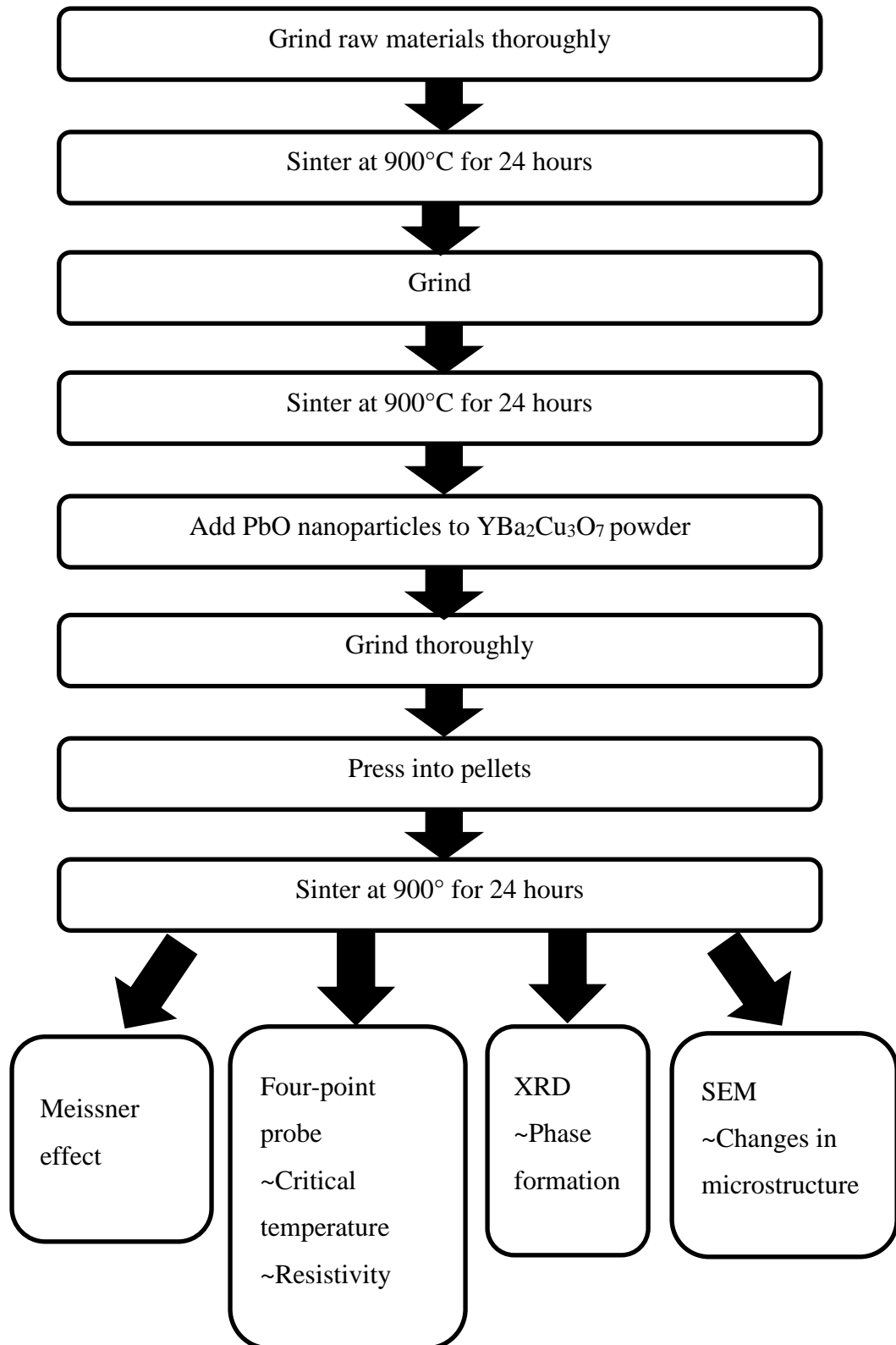


*Figure 3. 1.*    Flow chart of methodology of the experiment
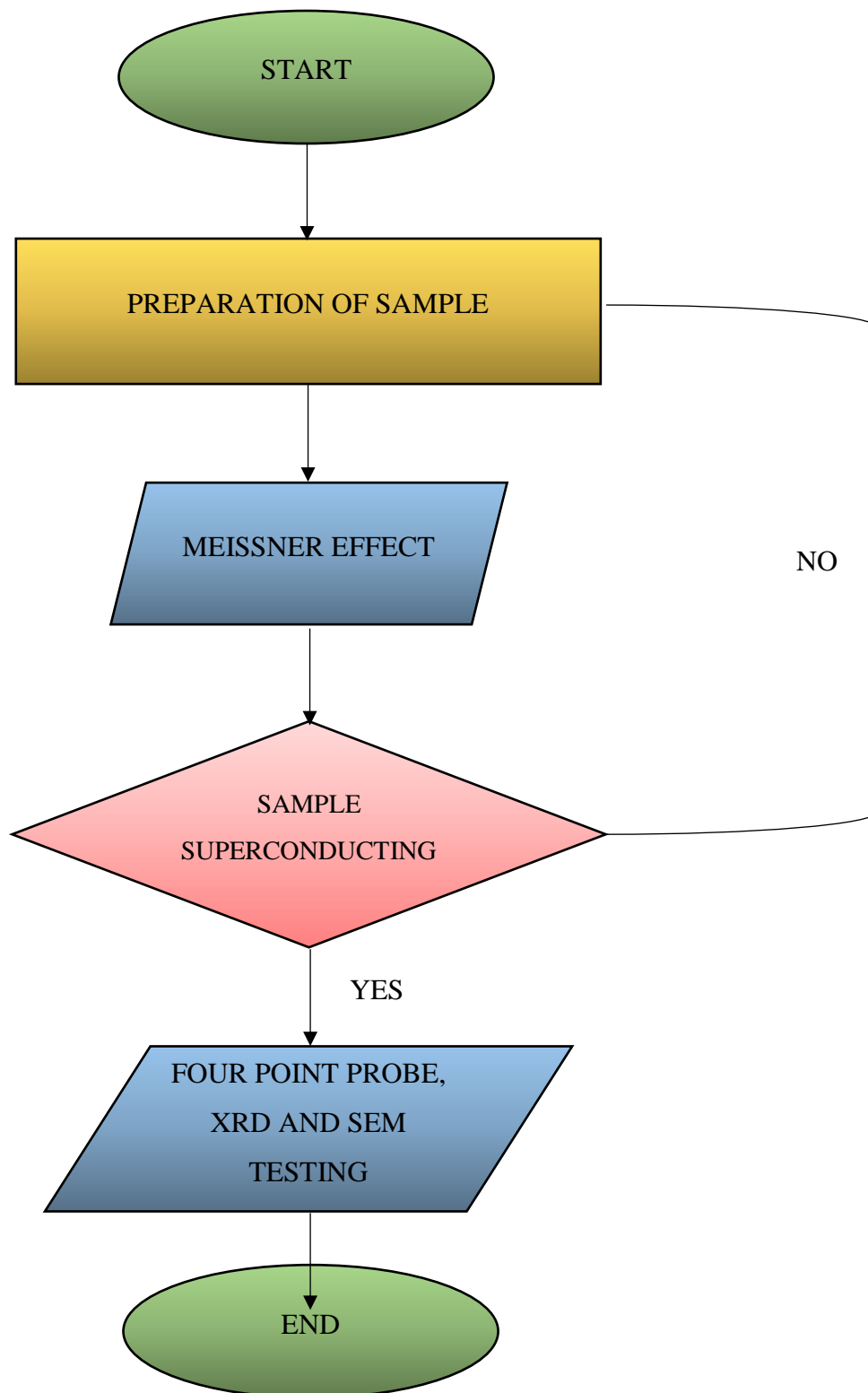
*Figure 3. 2.*     Procedure for characterization of sample

## 3.3 Material And Apparatus

### 3.3.1 List Of Chemicals And Materials

Chemicals and materials used in this research are listed below:

Table 3. 1.
*List of Materials and Chemicals used*

| No | Materials and Chemicals | Quantity |
|----|-------------------------|----------|
| 1 | Yttrium Oxide, $Y_2O_3$ (powder) purity | 7.55g |
| 2 | Barium Carbonate, $BaCO_3$ (powder) purity | 26.45g |
| 3 | Copper Oxide, CuO (powder) purity | 16g |
| 4 | Lead Oxide, PbO (powder) purity | 0.01g |
| 5 | Liquid Nitrogen | - |
| 6 | Silver Conducting Paint to attach pellets to wires | - |
| 7 | Ethanol for cleaning apparatus and equipment | - |
| 8 | Hydrochloric Acid for removing stains and residue from crucible | - |

### 3.3.2 List Of Apparatus And Equipment

Apparatus used for sample preparation are listed below:

Table 3. 2.
*List of apparatus and equipment used for sample preparation*

| No. | Materials and Chemicals | Quantity |
|-----|-------------------------|----------|
| 1 | Weighing Balance | 1 |
| 2 | Mortar and Pestle for grinding raw materials | 1 |
| 3 | Spatula | 1 |
| 5 | Furnace | 1 |
| 6 | Hydraulic Press and Pellet Mould | 1 |
| 7 | Vials | 5 |
| 8 | Crucible Bowl | 5 |

Equipment and apparatus used to characterize the samples are listed below

Table 3. 3.
*List of apparatus and equipment used for sample characterization*

| No. | Materials and Chemicals | Quantity |
|---|---|---|
| 1 | Scanning Electron Microscope | 1 |
| 2 | X-ray Diffraction | 1 |
| 3 | Strong Magnet | 1 |
| 4 | Retort stand | 1 |
| 5 | Heat Shrink Tape | 1 |
| 6 | Wires (Blue, Red, Black, Yellow) | 4 |
| 7 | Type T Thermocouple | 1 |

## 3.4    Sample Preparation

### 3.4.1    Solid State Reaction Method

The $YBa_2Cu_3O_7$ superconductor powder in this study was prepared by solid state reaction technique as is typically employed when preparing polycrystalline material. Cave et al., 2007 defines the process as a reaction between or within solid reactants to yield a solid product. Solid state reaction was chosen as the method of choice as limited to no side products will be form. (G. Kaupp, 2003) Besides that, no solvents will be required and hence waste disposal of solvent is not an issue.

The experimental procedure of solid state reaction begins with the mixing or grinding of the solid reactants. Grinding is used to break the materials into smaller particles and homogenize the mixture. After weighing the reactants to the accurate amount, several ways can be used to mix the reactants. One of which is by manual grinding using a mortar and pestle. Other alternatives that can be used for grinding are vortexes, glass homogenizers, ultrasonic treatment, and bead or grain mills. However, the use of mortar and pestle can bring about several disadvantages. Contamination is very

likely to occur. In order to prevent contamination, the mortar and pestle, spatula, and vials should be cleaned before using them for a new sample.

The next procedure of solid state reaction is sintering the mixed sample. Sintering is a process whereby heat is applied to agglomerate the metal particles. Sintering is commonly used to synthesise and consolidate advance materials such as superconductors. During the sintering process, intergranular contacts and subsequently necks between the particles are formed. The density of the aggregate may increase and continuous sintering causes further necking and densification. The determination of sintering temperature is dependent on the powder characteristics as well as the grain-size distribution, volume fraction and formation of contact region of the aggregate. (V.V Mitic et al., 2011)

In this research, the amount of raw materials used was calculated balanced chemical equation to be 7.55 g yttrium oxide ($Y_2O_3$), 26.45 g barium carbonated ($BaCO_3$) and 16.0 g copper oxide (CuO) for a total of 50 g. Using a mortar and pestle, the raw materials was grinded until all traces of white powder of yttrium oxide disappears. This was then followed by the sintering process in a furnace at 900°C for 24 hours with a heating time of 1 hour 30 minutes. (R. Abd-Shukor et al., 2014)

Then, the sample was removed from the furnace and grinded further to ensure homogeneity. After sintering a second time, at 900°C for 24 hours with a heating time of 1 hour 30 minutes, the sample was then divided into 5 equal parts and 0.00 wt%, 0.01 wt%, 0.02 wt%, 0.03 wt% and 0.04 wt% lead oxide (PbO) nanoparticle was added respectively. 10 g of the sample was sintered to be sent for XRD analysis while the other 40 g was pressed into pellets for further analysis.

### 3.4.2   Pelletization

Pelletization by definition is an agglomeration process to form spherical units called pellets from fine powder. (M. Hirjau et al., 2011). Pellet preparation involves a pellet mould and a hydraulic press to introduce mechanical stress that allows the fine powder to be pressed into pellets. An anvil is first placed inside a die chamber and filled with pre-measured sample. The sample is then covered with another anvil followed by

the plunger. The hydraulic press is utilized to compress the entire assembly with a suitable force. The pellet is then extracted.

In the case of this research, the pellet mould has a diameter of approximately 12.0 mm. 1.5 g of YBCO with the addition of 0.00 wt%, 0.01 wt%, 0.02 wt%, 0.03 wt% and 0.04 wt% PbO nanoparticle respectively was added into the pellet mould and placed into the hydraulic press. The hydraulic press was then put under pressure with a force of 25 kg/cm$^3$ for 35 seconds. The pellets were then sintered at 900°C for 24 hours with a heating time of 1 hour 30 minutes. The pellets form has a diameter of approximately 12 mm and 2.9 mm in thickness.

Table 3. 4.
*The weight, thickness and diameter of each pellet after sintering*

| Sample | | Weight (g) | Thickness (mm) | Diameter (mm) |
|---|---|---|---|---|
| YBCO + 0.01wt% | Pellet 1 | 1.473 | 2.973 | 12.472 |
| | Pellet 2 | 1.457 | 2.948 | 12.228 |
| YBCO + 0.02wt% | Pellet 1 | 1.460 | 2.979 | 12.740 |
| | Pellet 2 | 1.480 | 2.989 | 12.820 |
| YBCO + 0.03wt% | Pellet 1 | 1.471 | 2.868 | 12.291 |
| | Pellet 2 | 1.473 | 2.878 | 12.295 |
| YBCO + 0.04wt% | Pellet 1 | 1.475 | 2.879 | 12.391 |
| | Pellet 2 | 1.479 | 2.908 | 12.416 |

## 3.2    Sample Characterization

### 3.2.1  X-Ray Diffraction (XRD)



*Figure 3. 3.*    X-ray Diffractometer

The principle purpose of X-ray diffraction is for determining the crystal structure of materials, phase identification, qualitative and quantitative analysis and to control the quality of raw materials and products. X-ray diffraction utilizes the concept of destructive and constructive interference when an x-ray beam hits an atom. A diffracted beam is therefore composed of scattered rays mutually reinforcing one another.

Relating to this research, the XRD machine used is the Rigaku Miniflex X-Ray Diffractometer. The X-ray is generated by Cu Kα radiation sifted bt a Ni channel and has a wavelength of 1.54Å. To ensure reflections from various (h,k,l) planes, the sample was packed to a flat surface onto a sample holder. It was then set to measure powder diffraction patterns in the range of 3° to 90° in two theta (2θ) scanning range, at the scan rate of 3°/min and with the step size of 0.02°.

### 3.2.2 Scanning Electron Microscopy (SEM)



*Figure 3. 4.* (a) Scanning electron microscope (b) Sputter coater

Scanning electron microscope is able to scan a sample with a focused beam to obtained images and information on the topography and composition of the sample. In a scanning electron microscope, an electron beam is generated in high vacuum by thermionic emission from a tungsten wire. Electromagnetic lenses then condense the electron beam and is transmitted through the sample. The image is then focused and projected onto a screen.

In this research, the SEM machine used is of the brand Carl-Zeiss. To begin, the sample was cracked slightly to observe the internal structure of the sample and then coated with a thin layer of platinum to improve the imaging of samples. The electron high tension (EHT) of the SEM was set to 8 kV and other appropriate parameters such as the magnification, contrast and aperture alignment was set. The detector chosen in this case was SE1 detector, which is commonly used for general purpose imaging.

### 3.2.3 Four Point Probe
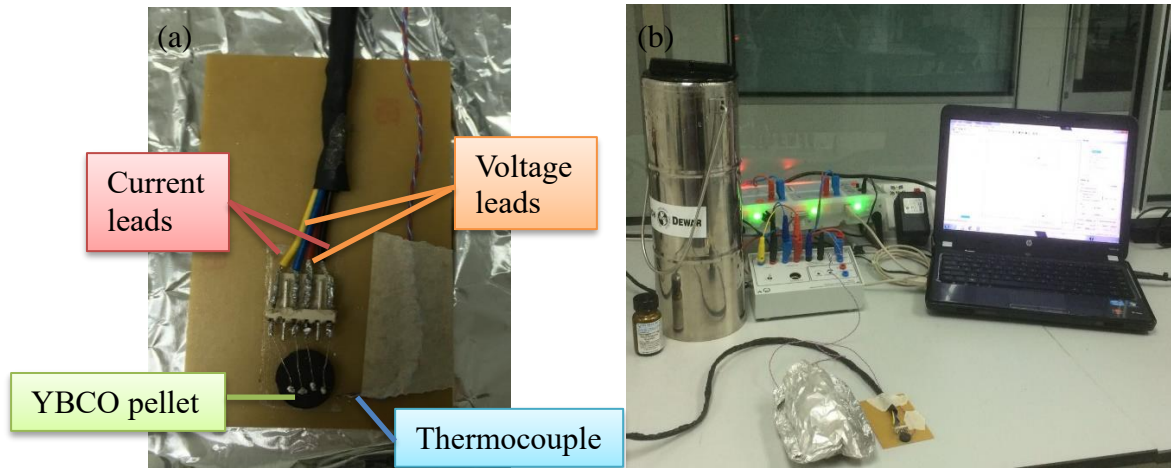


*Figure 3. 5.*    (a) Four-point probe (b) Experimental set-u p to test for critical temperature

The four-point probe was constructed to test the critical temperature of the superconductor. Four wires of varying colours (Black, Yellow, Blue and Red) was cut to equal length of 2 m, attached to banana plugs and fed through a heat shrink tube. The exposed wires were then attached permanently soldered onto an electrical connector. Two wires (Black and Yellow) were attached to the far end of the connectors whereas the other two wires (Red and Blue) were attached to the inner points of the connectors. Four single strand of wires were also soldered on the other end of the electrical connector.

The two outer wires were then connected to a current source and the inner wires was connected to a voltmeter to obtain a voltmeter reading. A thermocouple was also attached to the voltmeter as well.

The electrical connector and pellet was attached to a board using double sided tape. The single strands of wires were connected to the pellet using silver connecting paint. The thermocouple was attached to pellet with tape as well. A current of 140 mA was applied to the pellet. The entire connection was then wrapped in aluminium foil and lowered very slowly into liquid nitrogen to ensure even cooling of the pellet. The whole system was measured by a Cassylab software on a laptop to measure the reading of voltage across the pellet as well as the voltage of the thermocouple.

### 3.5.4 Meissner Effect

Meissner effect is the phenomenon when a superconductor at its critical temperature repels the magnetic field. This causes the superconductor to levitate above a magnet showing positive superconductivity.

In this case, the magnet use is Neodymium magnet. The magnets were arranged in rows of two to ensure even distribution of magnetic field. Each magnet has a size of 1.5mmx6.5mmx2.0mm and has a strength of 1.175T. The superconductor pellet was first immersed in liquid nitrogen and after several seconds, it was removed and placed on the magnet. The duration of the levitation was recorded and analysed.

.

# CHAPTER 4

# RESULT AND DISCUSSION

## 4.1    Microstructure Analysis

### 4.1.1   X-Ray Diffraction (XRD) Analysis

Figure 4.1 to figure 4.4 shows the XRD patterns of YBCO with the addition of 0.00 wt%, 0.01 wt%, 0.02 wt%, 0.03 wt% and 0.04 wt% PbO respectively. Figure 4.5 shows the normalized graph of YBCO with the addition of varying amount of PbO nanoparticle. The lattice parameter of each sample are summarized in Table 4.1.

When oxygen vacancies are present in the copper layer of the structure, YBCO has a tetragonal structure that is insulating and non-superconducting. However, in excess oxygen, the oxygen sites are occupied causing an elongation in of the *b* axis of the lattice parameter and hence distorting the shape of the structure from a tetragonal to an orthorhombic structure.

Using the information obtained via the XRD analysis, the lattice parameter of the structure can be calculated as follow.

$$\frac{1}{d^2} = \frac{h^2}{a^2} + \frac{k^2}{b^2} + \frac{l^2}{c^2}$$
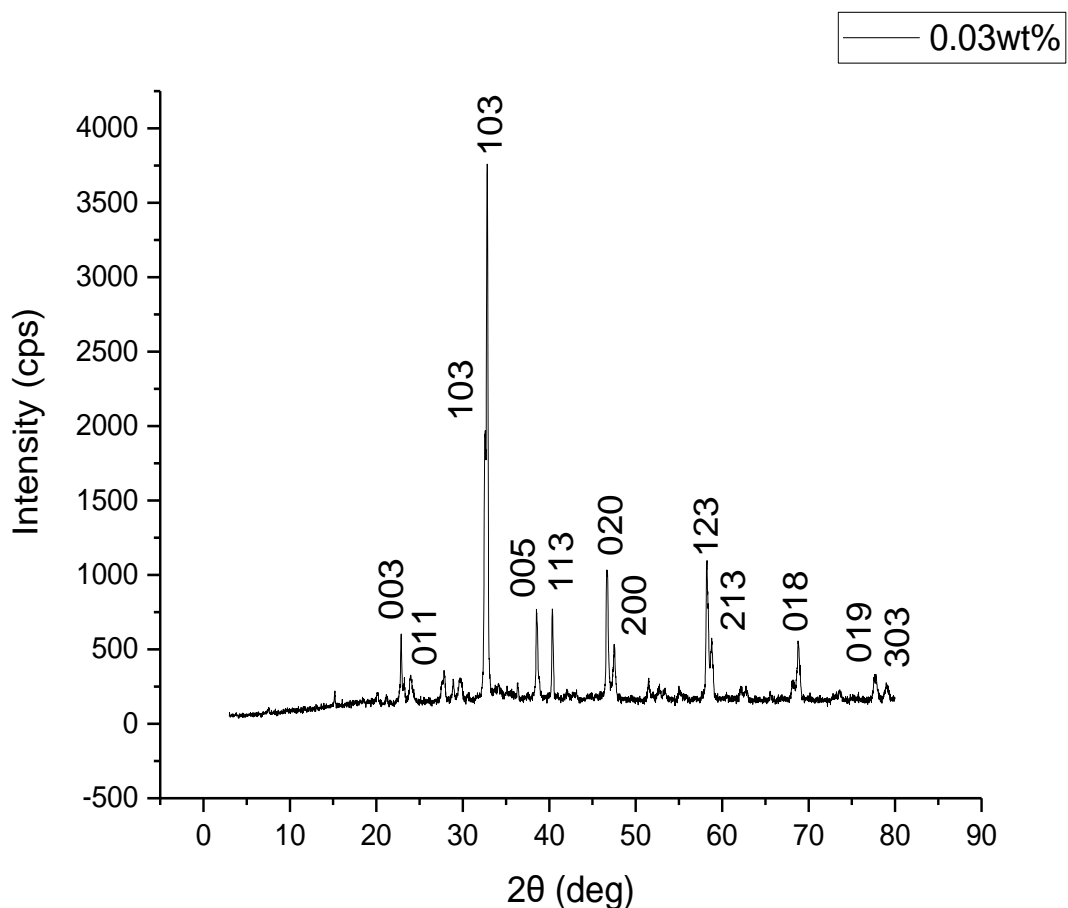
Eq (4.1)
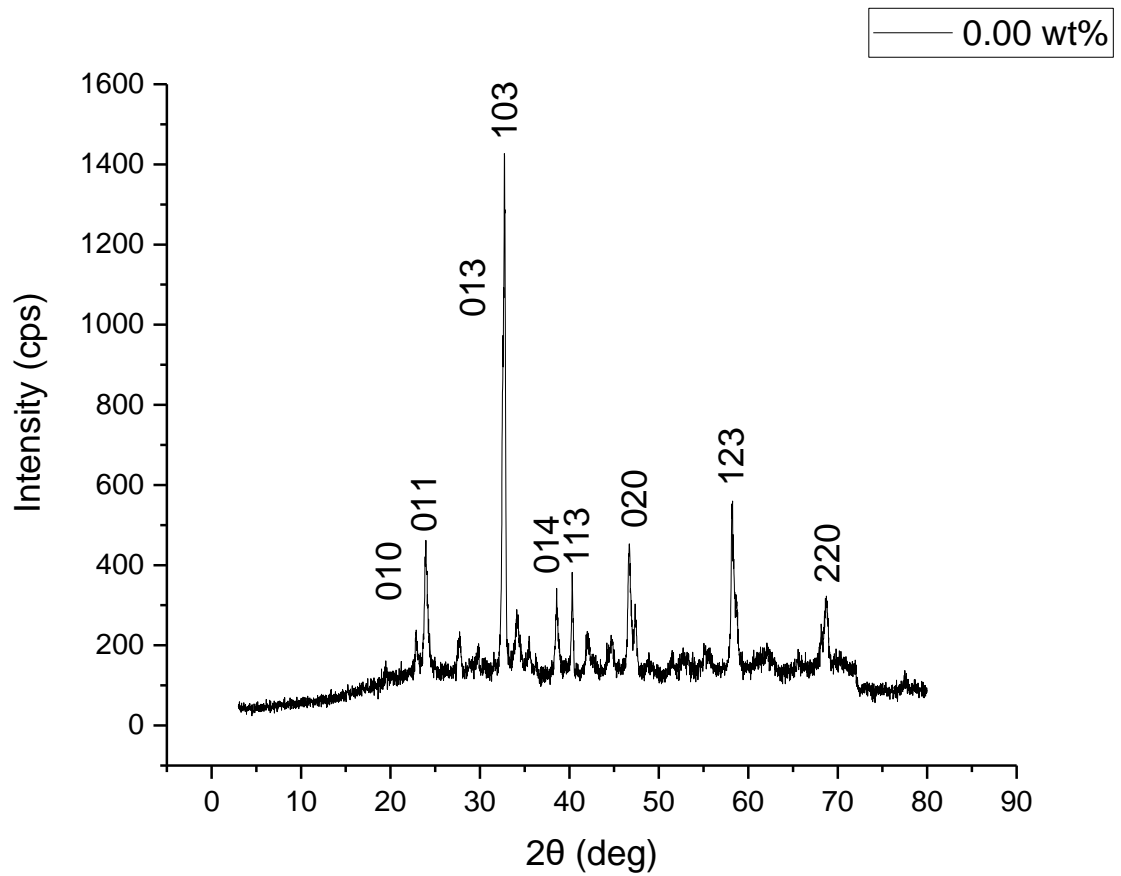
*Figure 4. 1.*    XRD spectra of YBCO with the addition of 0.00 wt% PbO with corresponding Miller indices of each peak

Figure 4.1 shows the XRD spectra of YBCO with the addition of 0.00 wt% PbO with corresponding Miller indices of each peak. The highest peak intensity recorded was 820 cps at 32.769° on the plane (1,0,3). The lattice parameter calculated for x = 0.00 w$t$% was $a = 3.83871$Å, $b = 3.8891$Å and $c = 11.644$Å.
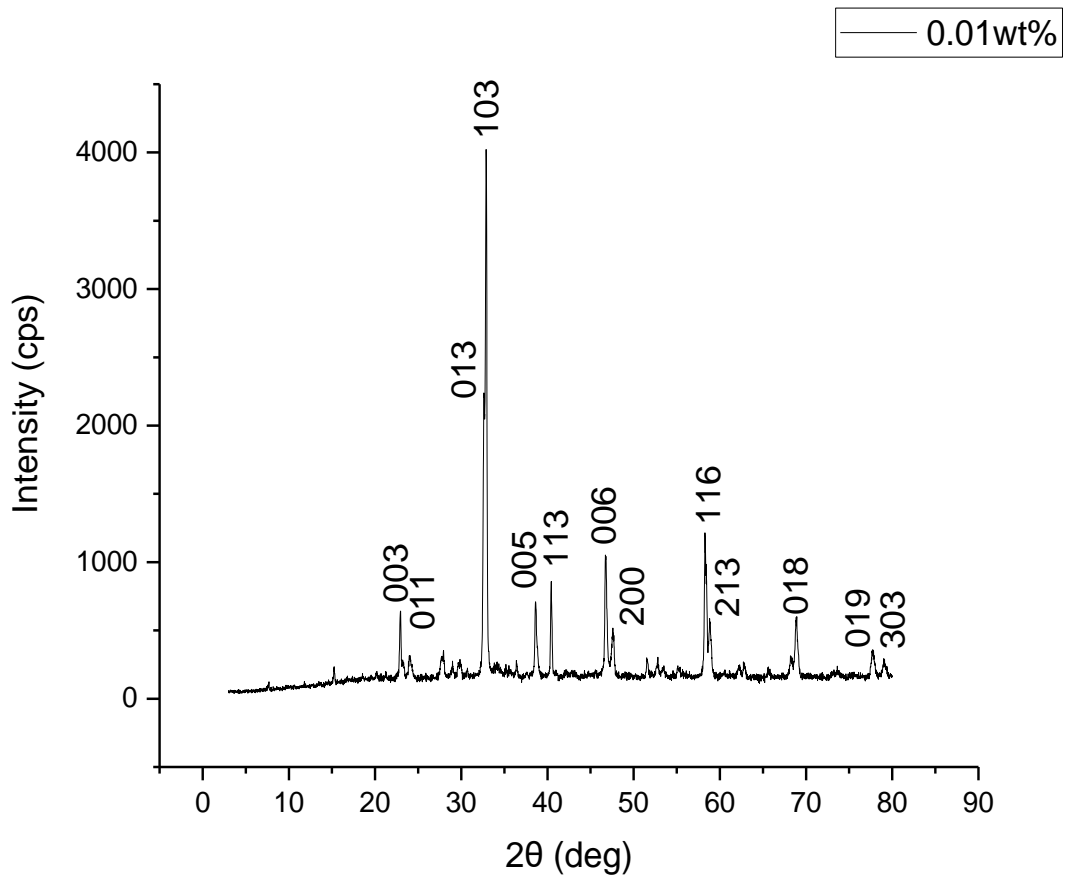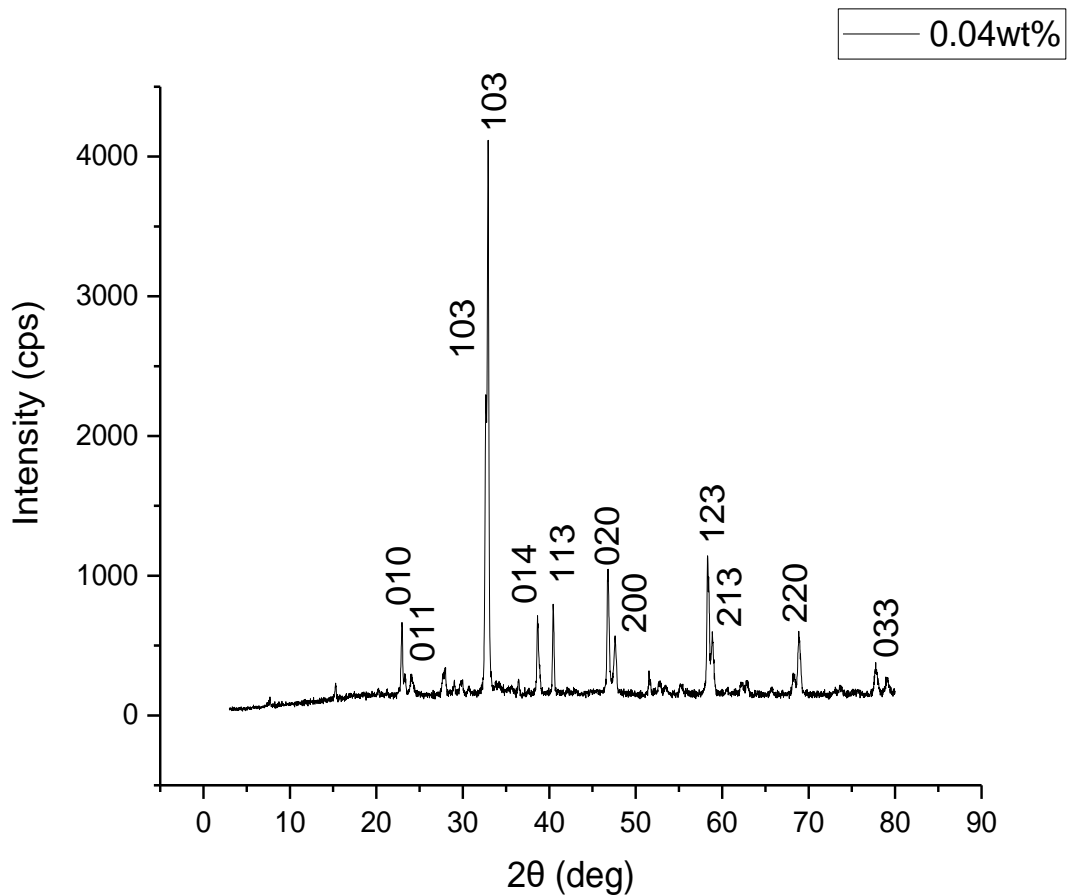
*Figure 4. 2.* XRD spectra of YBCO with the addition of 0.01 wt% PbO with corresponding Miller indices of each peak

Figure 4.2 shows the XRD spectra of YBCO with the addition of 0.01 wt% PbO with corresponding Miller indices of each peak. The highest peak intensity recorded was 2883 cps at 32.880° on the plane (1,0,3), followed by the second highest peak at 1412 cps at 32.619° on the plane (0,1,3). No obvious PbO peak was detected in the sample as the addition of the nanoparticle was not significant enough. The lattice parameter calculated for x = 0.01w$t$% was $a = 3.8721$Å, $b = 3.8291$Å and $c = 11.618$Å.
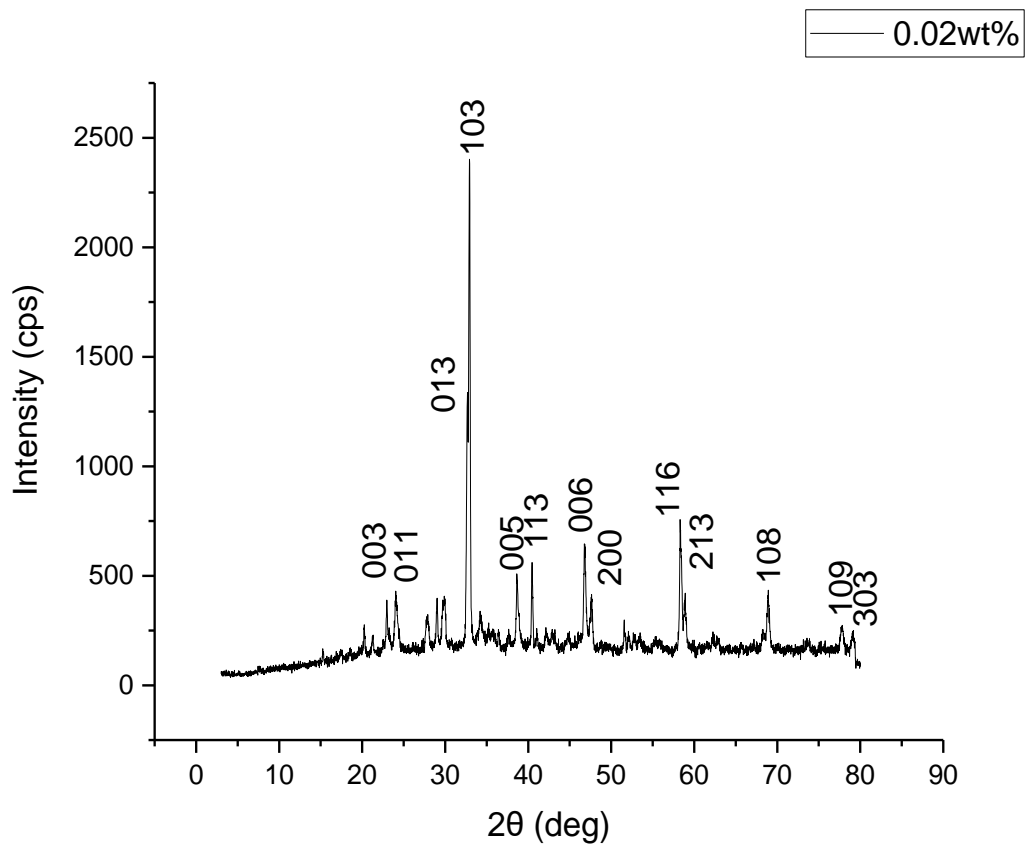
*Figure 4. 3.* XRD spectra of YBCO with the addition of 0.02 wt% PbO with corresponding Miller indices of each peak

Figure 4.3 shows the XRD spectra of YBCO with the addition of 0.02 wt% PbO with corresponding Miller indices of each peak. The highest peak intensity recorded was 1722 cps at 32.910° on the plane (1,0,3), followed by the second highest peak at 818 cps at 32.667° on the plane (0,1,3). No obvious PbO peak was detected in the sample as the addition of the nanoparticle was not significant enough. The lattice parameter calculated for x = 0.02w$t$% was $a = 3.8750$Å, $b = 3.8158$Å and $c = 11.619$Å.

*Figure 4. 4.*    XRD spectra of YBCO with the addition of 0.03 wt% PbO with corresponding Miller indices of each peak

Figure 4.4 shows the XRD spectra of YBCO with the addition of 0.03 wt% PbO with corresponding Miller indices of each peak. The highest peak intensity recorded was 2726 cps at 32.812° on the plane (1,0,3), followed by the second highest peak at 1259 cps at 32.550° on the plane (0,1,3). No obvious PbO peak was detected in the sample as the addition of the nanoparticle was not significant enough. The lattice parameter calculated for x = 0.02w$t$% was $a = 3.8228$Å, $b = 3.8930$Å and $c = 11.679$Å.

*Figure 4. 5.*    XRD spectra of YBCO with the addition of 0.04 wt% PbO with corresponding Miller indices of each peak

Figure 4.4 shows the XRD spectra of YBCO with the addition of 0.04 wt% PbO with corresponding Miller indices of each peak. The highest peak intensity recorded was 2906 cps at 32.915° on the plane (1,0,3), followed by the second highest peak at 1480 cps at 32.650° on the plane (0,1,3). No obvious PbO peak was detected in the sample as the addition of the nanoparticle was not significant enough. The lattice parameter calculated for x = 0.04w$t$% was $a = 3.8164$Å, $b = 3.877$Å and $c = 11.6578$Å.
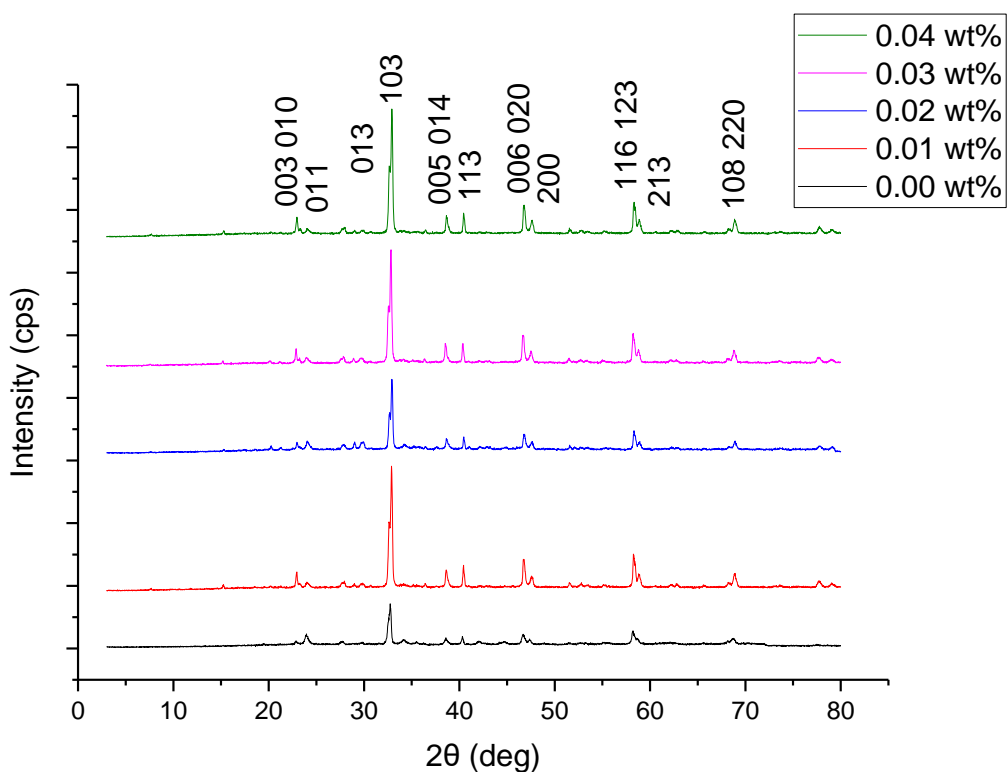
*Figure 4. 6.* XRD pattern for normalized graph of YBCO with the addition of varying amount of PbO nanoparticle with corresponding Miller indices of each peaks

Figure 4.5 is the normalized graph of YBCO with the addition of varying amount of PbO nanoparticle. From the graph, it is observed that the XRD pattern and peaks of the samples remained relatively similar with the highest peak intensity to be at approximately 32.8° on the (0,1,3) plane. The addition of PbO nanoparticle shows little to no impact on the composition of the sample due to its insignificant amount.

Table 4. 1.
*Lattice parameter for each sample*

| Sample | a (Å) | b (Å) | c (Å) |
|---|---|---|---|
| YBCO + 0.00wt% PbO | 3.8387 | 3.8890 | 11.644 |
| YBCO + 0.01wt% PbO | 3.8721 | 3.8291 | 11.618 |
| YBCO + 0.02wt% PbO | 3.8750 | 3.8158 | 11.619 |
| YBCO + 0.03wt% PbO | 3.8228 | 3.8930 | 11.679 |
| YBCO + 0.04wt% PbO | 3.8164 | 3.8770 | 11.657 |

From the calculation of the lattice parameter, all samples show that it has an orthorhombic structure where $a \neq b \neq c$. The therefore assumed that superconductivity is not destroyed by the addition of PbO nanoparticles.

### 4.1.2 Scanning Electron Microscopy (SEM)

There were cracks on the non-added sample presumably due to its surrounding humidity which have hindered further experimentation and analysis. Hence, the following results is compared only between the samples with varying amount of PbO nanoparticles.

Scanning electron microscopy was used to determine and analyse the surface morphology of the samples. Figure 4.7 shows the SEM mircrograph for samples with 0.01 wt% PbO nanoparticle at a magnification of 300x, 500x, 800x and 1000x. Figure 4.8 shows the SEM mircrograph for samples with 0.02 wt% PbO nanoparticle at a magnification of 300x, 500x, 800x and 1000x. Figure 4.9 shows the SEM mircrograph for samples with 0.03 wt% PbO nanoparticle at a magnification of 300x, 500x, 800x and 1000x. and figure 4.10 shows the SEM mircrograph for samples with 0.04 wt% PbO nanoparticle at a magnification of 300x, 500x, 800x and 1000x.

The black areas are pores whereas the grey areas are randomly oriented superconducting crystals. All the samples showed dense microstructure with minimal porosity. In addition to that, the results also show that the samples have an irregular surface and irregular pore size and shape. Previous research has showed that the addition of nanoparticles as impurities may cause an increase in porosity. (S. Terzieva et al., 2005).
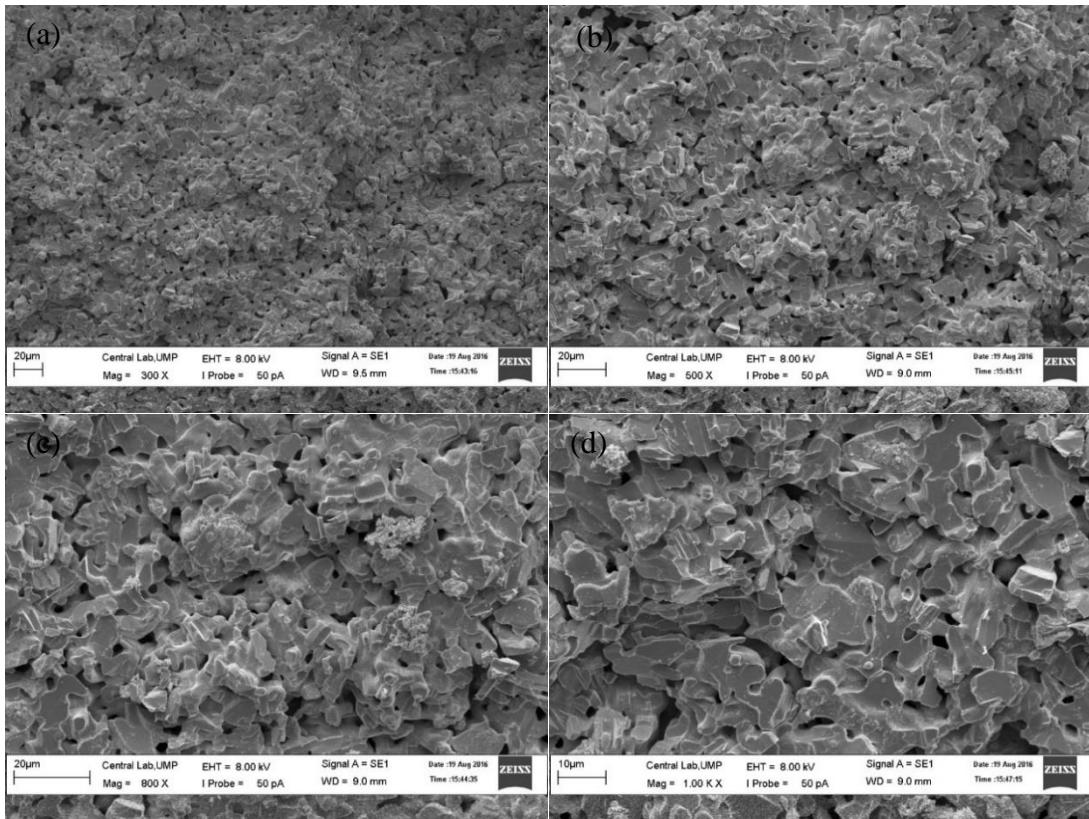
*Figure 4. 7.* SEM micrograph of YBCO with the addition of 0.01 wt% PbO nanoparticle at (a) 300x, (b) 500x, (c) 800x and (d) 1000x magnification
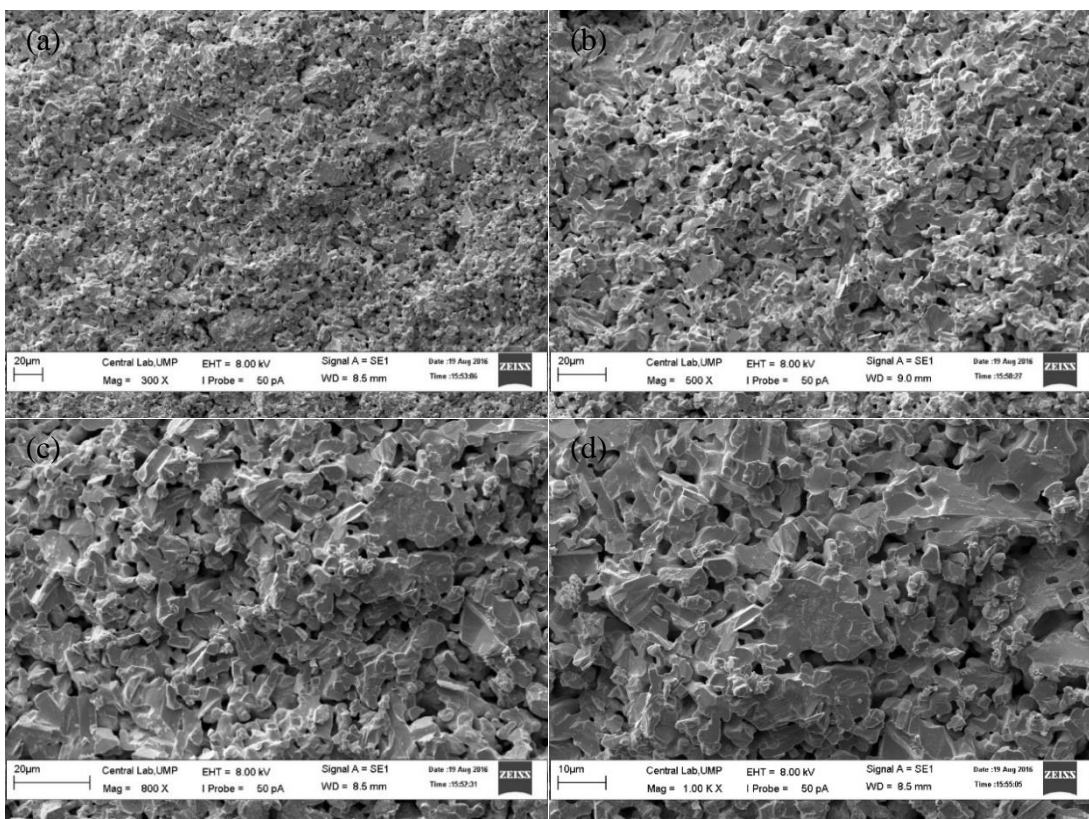


*Figure 4. 8.* SEM micrograph of YBCO with the addition of 0.02 wt% PbO nanoparticle at (a) 300x, (b) 500x, (c) 800x and (d) 1000x magnification
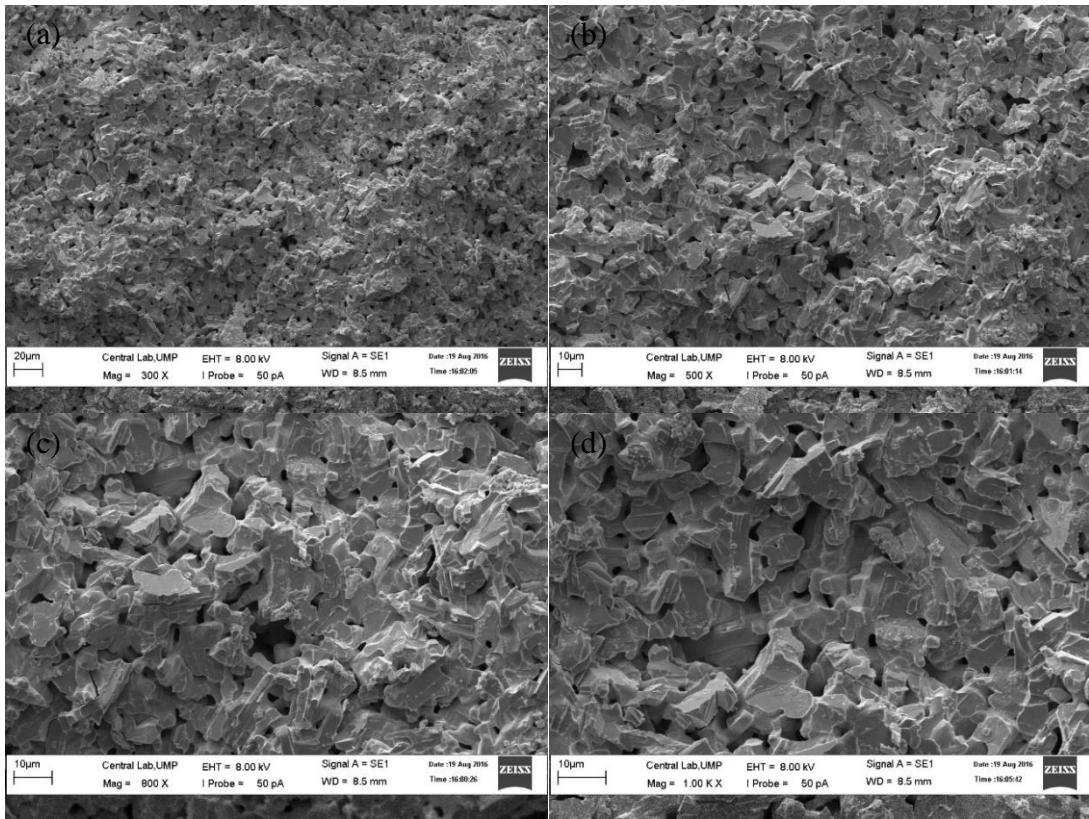
*Figure 4. 9.* SEM micrograph of YBCO with the addition of 0.03 wt% PbO nanoparticle at (a) 300x, (b) 500x, (c) 800x and (d) 1000x magnification
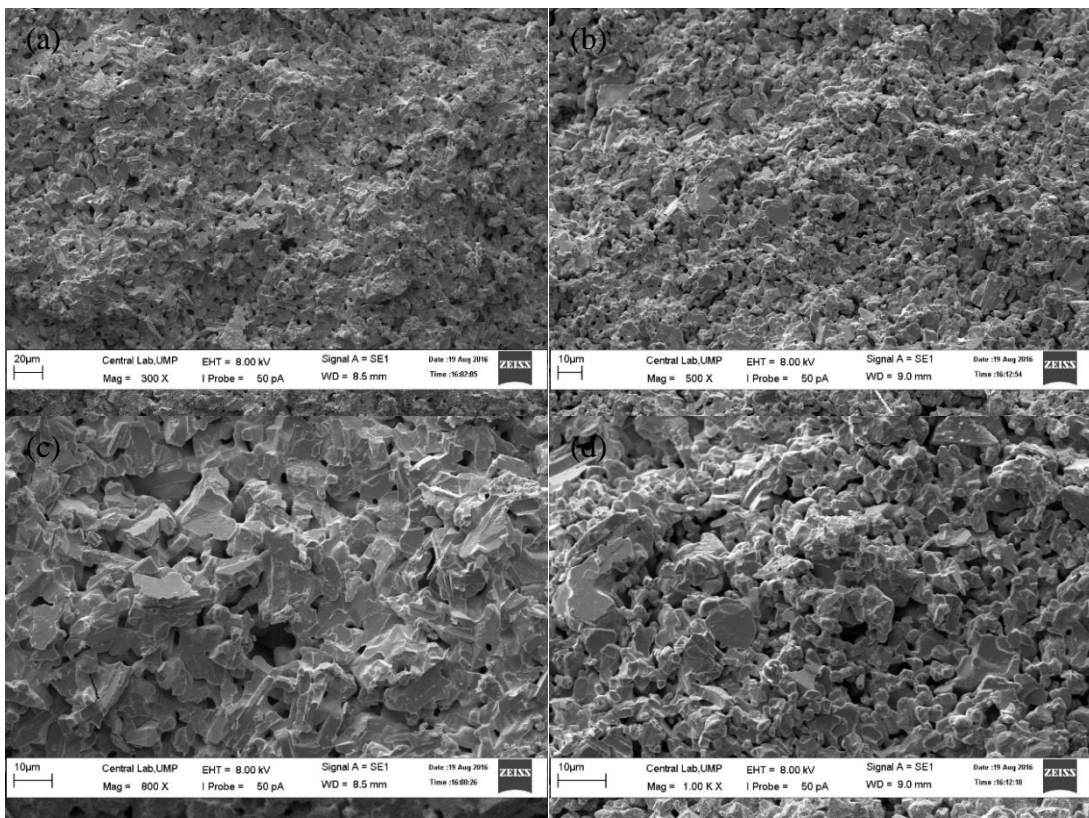


*Figure 4. 10.* SEM micrograph of YBCO with the addition of 0.04 wt% PbO nanoparticle at (a) 300x, (b) 500x, (c) 800x and (d) 1000x magnification

## 4.2    Electronic Properties Analysis

### 4.2.1    Meissner Effect Analysis



*Figure 4. 11.*    YBCO pellet showing Meissner effect

The sample levitates above a magnet due to Meissner effect. Table 4.2 shows the recorded levitation time of each sample above a row of Neodymium magnets before it drops. The levitation is an indication of superconductivity of the samples at its critical temperature. Once the samples are no longer at its critical temperature, Meissner effect cease to occur.

Table 4. 2.
*Levitation time for each sample*

| Sample | Time 1 (s) | Time 2 (s) | Time 3 (s) | Average (s) |
| --- | --- | --- | --- | --- |
| YBCO + 0.00wt% PbO | <2 | <2 | <2 | <2 |
| YBCO + 0.01wt% PbO | <2 | <2 | <2 | <2 |
| YBCO + 0.02wt% PbO | 11.48 | 15.39 | 14.85 | 13.91 |
| YBCO + 0.03wt% PbO | 21.62 | 21.73 | 20.31 | 21.22 |
| YBCO + 0.04wt% PbO | 23.53 | 25.36 | 25.04 | 24.65 |

The non-added sample as well as the sample with 0.01wt% addition shows a levitation time of less than 2 seconds whereas the sample with 0.04 wt% addition has the longest levitation time.

The levitation time of sample in this case is not an accurate indication of the critical temperature. This is because when the sample is submerged into liquid nitrogen, it is assumed that it is at its critical temperature. However, when the sample is removed from liquid nitrogen to be transferred to the magnet, its temperature slowly rises until it is no longer at critical temperature. The rate at which each sample is heated to room temperature may not be the same. A four point probe analysis was therefore conducted to obtained a more accurate reading of its critical temperature.

## 4.2.2   Four Point Probe Analysis

Although there may be inaccuracies in the reading from the four-point probe analysis, an estimated reading was able to be obtained and can serve as an early indication of the effect of nanoparticle addition on the superconductor. Due to faulty voltage reading, the critical temperature of the sample was difficult to obtain and hence appeared to lower the critical temperature instead of increasing it. The measurement and analysis of current density of the superconductor sample was not carried out due to similar reasons.
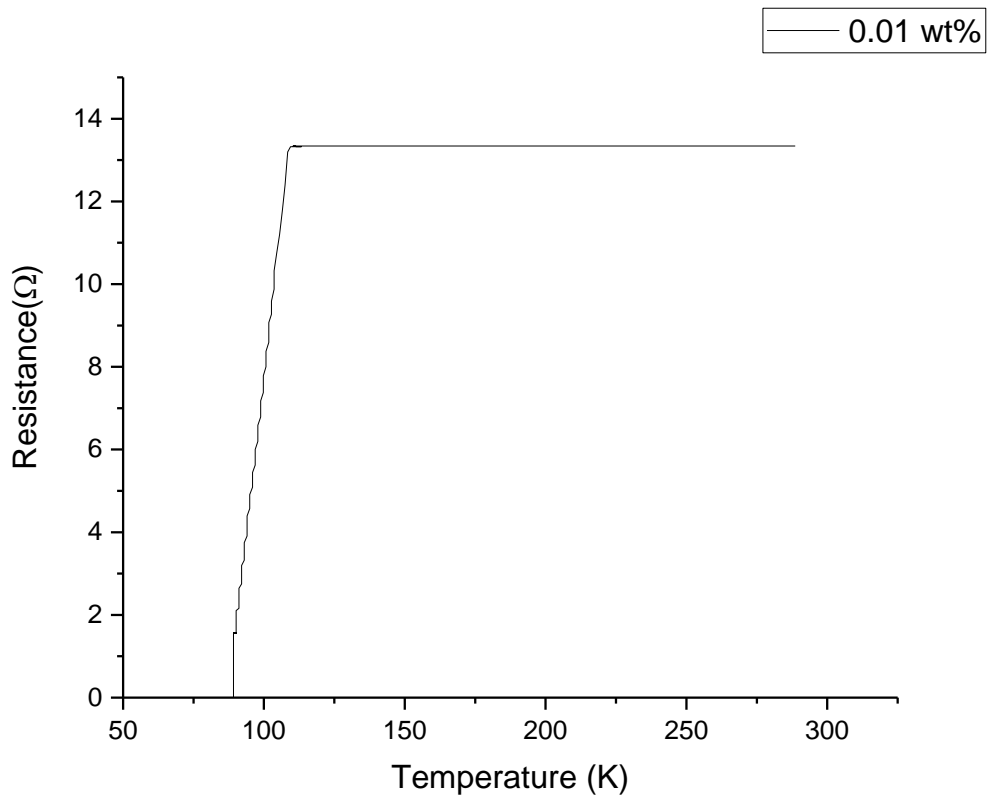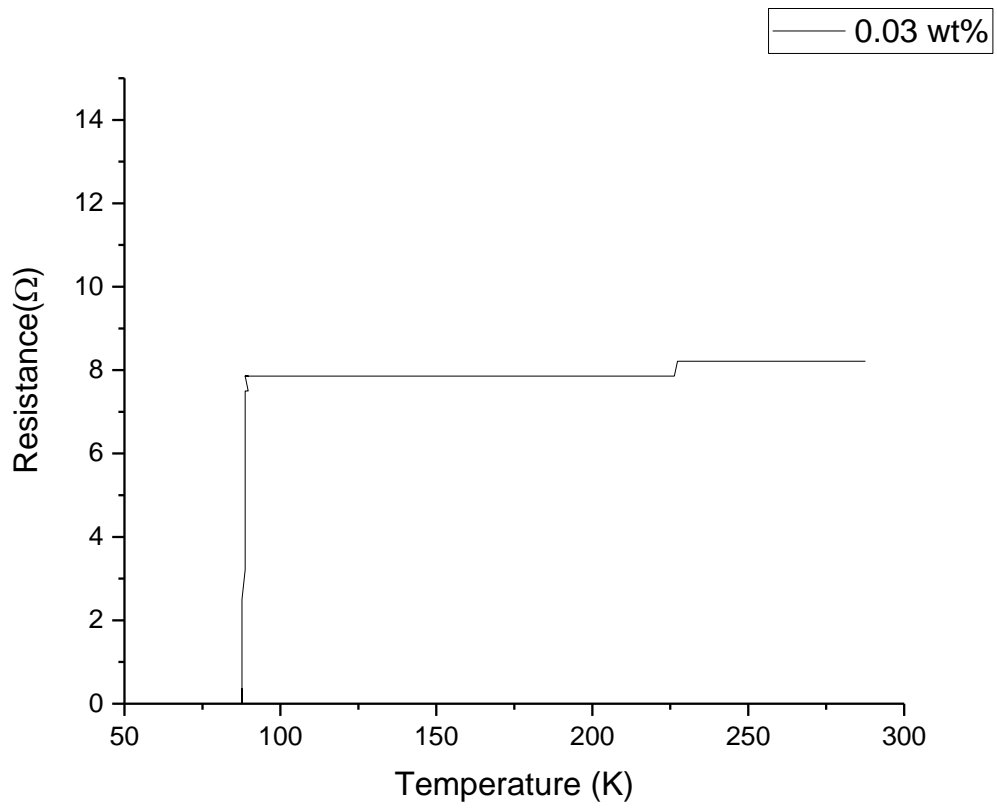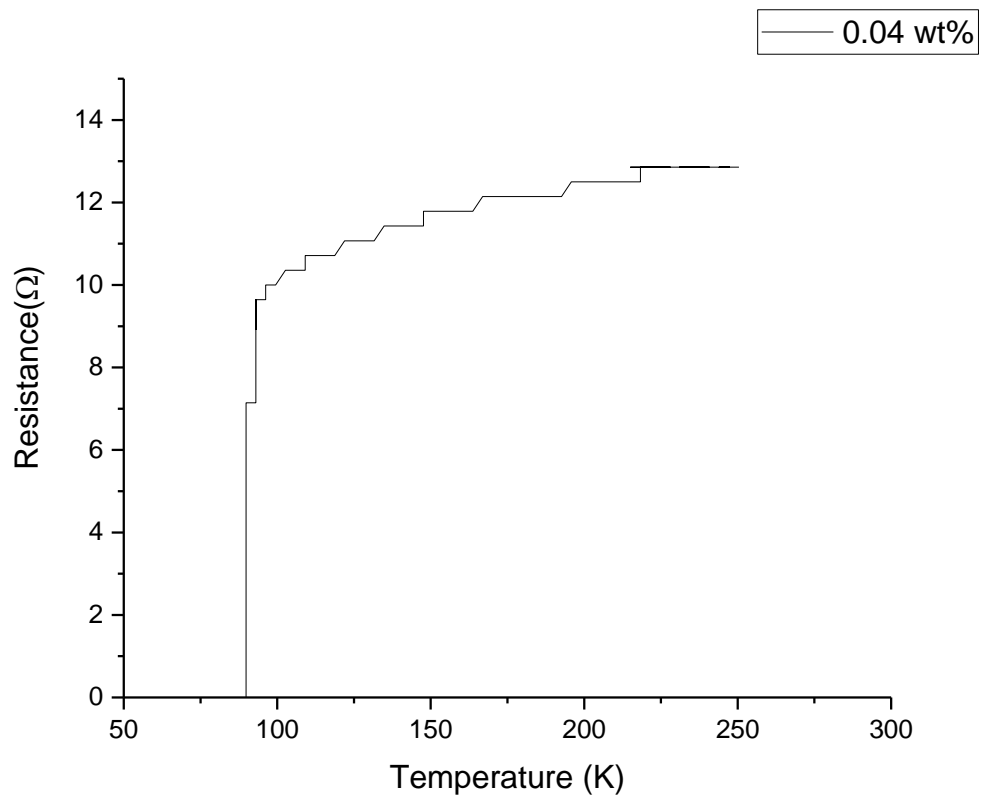
*Figure 4. 12.* Resistance against temperature graph for YBCO with the addition of 0.01 wt% PbO nanoparticle.

From the graph, it is observed that the resistance drops abruptly from 13.0 Ω to 0 Ω when the temperature reaches 88.67 K.
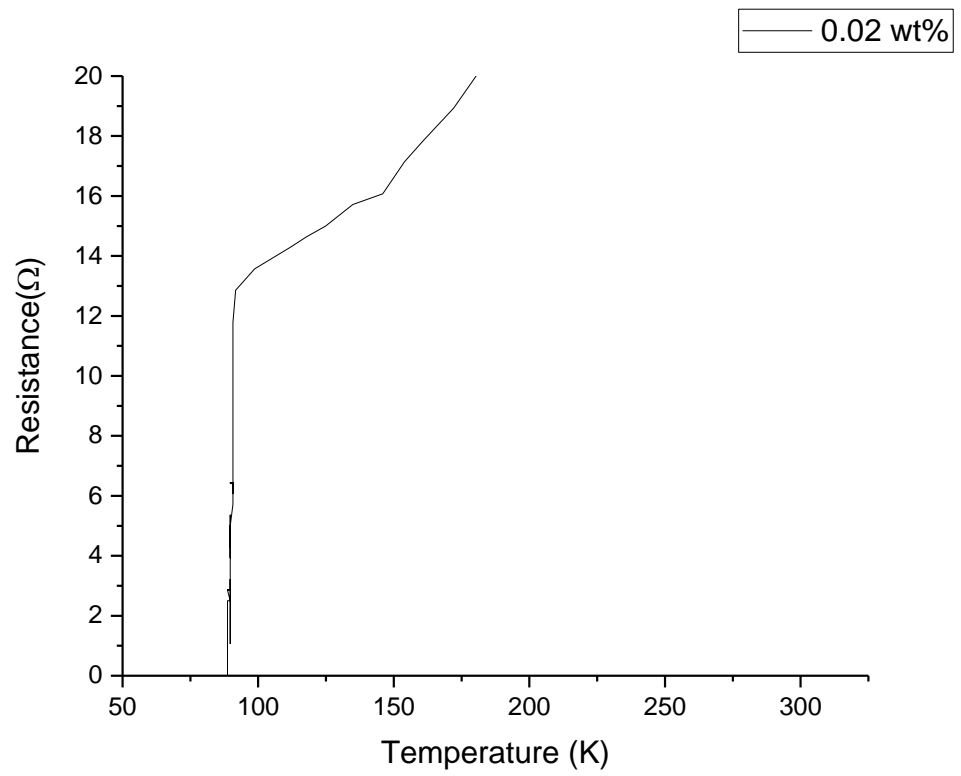
*Figure 4. 13.* Resistance against temperature graph for YBCO with the addition of 0.02 wt% PbO nanoparticle.

From the graph, it was observed that the resistance drops abruptly from 13.4 Ω to 0 Ω when the temperature reaches 89.18 K.

*Figure 4. 14.* Resistance against temperature graph for YBCO with the addition of 0.03 wt% PbO nanoparticle.

From the graph, it is observed that the resistance drops abruptly from 7.85 $\Omega$ to 0 $\Omega$ when the temperature reaches 87.67 K.

*Figure 4. 15.* Resistance against temperature graph for YBCO with the addition of 0.04 wt% PbO nanoparticle.

From the graph, it is observed that the resistance drops abruptly from 12.88 Ω to 0 Ω when the temperature reaches 89.82 K.
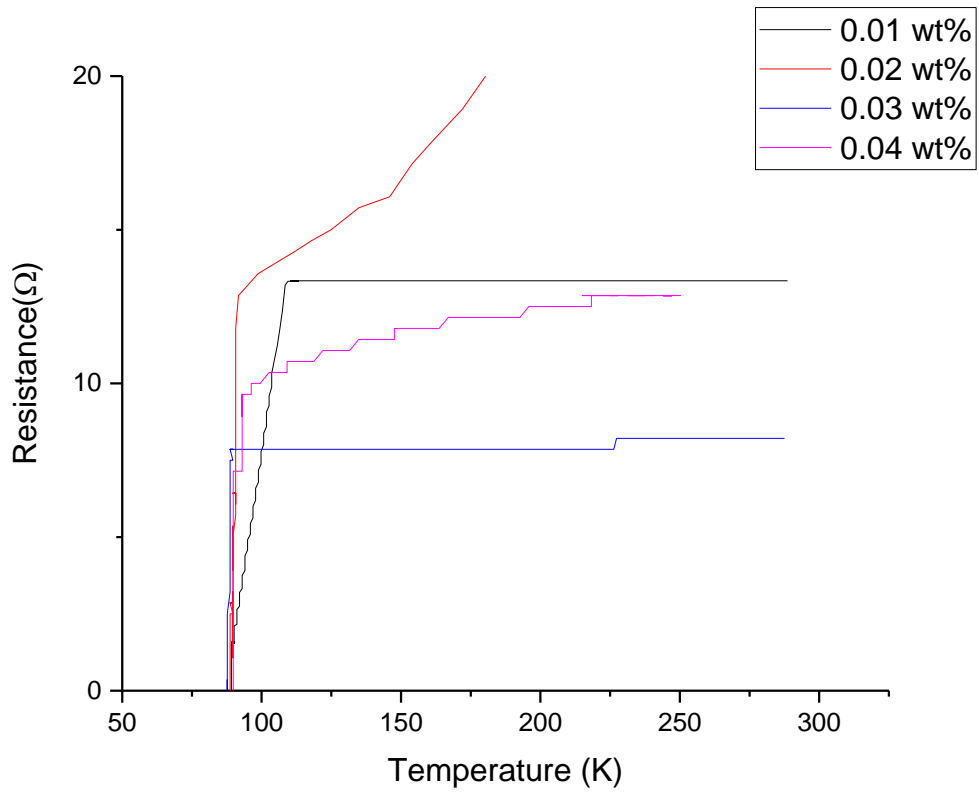
*Figure 4. 16.* Resistance against temperature graph for YBCO with the addition of varying amounts of PbO nanoparticle.

Table 4. 3.
*Critical temperature for each sample*

| Sample | Critical Temperature, $T_c$ (K) |
|---|---|
| YBCO + 0.01wt% PbO | 88.67 |
| YBCO + 0.02wt% PbO | 89.18 |
| YBCO + 0.03wt% PbO | 87.67 |
| YBCO + 0.04wt% PbO | 89.82 |

Based on the graph of resistance against temperature for YBCO with the addition of varying amounts of PbO nanoparticle and the table of sample with its corresponding critical temperature, the addition of 0.04 wt% of PbO nanoparticle to YBCO showed the highest critical temperature followed by 0.02 wt% addition, 0.01 wt% addition and finally 0.03 wt% addition. Hence, the critical temperature somewhat increases as the

nanoparticle addition increases with the exemption of 0.03 wt% nanoparticle addition. This shows that further increment in critical temperature is possible with increasing amount of nanoparticle. Therefore, subsequent research can be conducted to further show the maximum amount of nanoparticle addition that can yield the highest critical temperature.

However, there may be inaccuracies in the reading due to multiple factors. Faulty equipment and lack of proper apparatus are some of the causes that may have contributed to the discrepancies. Besides that, the samples may have impurities or contamination that will affect the performance of its superconductivity.

# CHAPTER 5

# CONCLUSION AND RECOMMENDATION

## 5.1　Conclusion

YBCO superconductor with the addition of PbO nanoparticle was successfully fabricated using solid state reaction method. The effect of nanoparticle addition on the phase formation and microstructure was studied using X-ray diffractometer and scanning electron microscope respectively. From the results, it was observed that there were no apparent changes between the non-added sample and the sample with the addition of nanoparticle. The small addition of nanoparticle was not significant enough to affect the microstructure and the phase formation of the YBCO sample

Meissner effect was also tested to study the presence of superconductivity. Levitation of sample above the neodymium magnet shows that the sample is superconducting. All samples which includes the non-added sample as well as the samples with the addition of varying amounts of nanoparticle show positive results when suspended over the magnet. The longest levitation time was studied to be for the sample with 0.04wt% nanoparticle addition with an average time of 24.65s. The levitation of the sample is an early indication that it has a higher critical temperature.

The critical temperature was determined using a four-point probe. Based on the results, it was observed that the highest critical temperature was for the sample with 0.04 wt% nanoparticle addition. However, a more accurate critical temperature could not be determined due to several errors in reading the voltage of the results.

**5.2     Recommendations**

The following are recommendation that can be done to improve the performance and results of the study:

1.      The pelletisation proved to be a challenge as the equipment and method used was not ideal to remove the pellets from the pellet mould. A pellet extruder should be included with the equipment to reduce defects or damages to the sample.

2.      The pellet should be kept with silica gel to avoid humidity. Humidity will cause the pellets to crack and break which may affect the testing of the pellets.

3.      A more proper and accurate reading of the voltage should be obtained with better and precise equipment and software, besides also proper understanding on the use and handling of the equipment.

4.      As the results of the experiment shows a continuous increase in critical temperature with the addition of nanoparticles until 0.04 wt% addition, further study need to be carried out in order to determine the highest amount of nanoparticle addition that can yield an increase in critical temperature.

.

# REFERENCE

Abd-Ghani, S.N., Abd Shukor, R., & Kong, W (2012). Effects of $Fe_3O_4$ Nanoparticles Addition in High Temperature Superconductor $YBa_2Cu_3O_{7-\delta}$. *Advanced Materials Research, 501, 309-313*

Abd-Shukor, R., Nazrin, M., Aisyah, I., Lee, W. K., Yusrianto, E., Jannah, A. N., & Halim S. A. (2014). Effect of nano-sized Co3O4 addition on the transport properties of $YBa_2Cu_3O_{7-\delta}$. *AIP Conf. Proc., 1574*, 268-273.

Abrikosov, A. (2003). Type II Superconductors and the Vortex Lattice. *Nobel Lecture*

Alecu, G. (2004). Crystal Structures of Some High-Temperature Superconductors. *Romanian Reports in Physics, 56*(3), 404-412.

Bardeen, J., Cooper, L., & Schrieffer, J. (1957). Free to Read Theory of Superconductivity. *Phys. Rev, 108*(5), 1175-1204.

Bennemann, K., & Ketterson, J. B. (2008) *History of Superconductor: Conventional, High Transition Temperature and Novel Superconductor*. Springer

Carter, C. B., & Norton, M. G. (2007). *Solid-State Phase Transformations and Reactions* (1st ed.). New York: Springer New York.

De Bruyn Ouboter, R. (1997). Heike Kamerlingh Onnes's Discovery of Superconductivity. *Scientific American, 276*(3), 98-103.

G. Kaupp, CrystEngComm. 23 (2003) 117.

G. W. Cave, C. L. Raston, J. L. Scott, Chem. Commun (2001) 2159-2169

Hafiz, M., & Abd-Shukor, M. (2015). Effect of Nanosized $NiF_2$ Addition on the Transport Critical Current Density of Ag-Sheathed $(Bi_{1.6}Pb_{0.4})Sr_2Ca_2Cu_3O_{10}$ Superconductor Tapes. *Advances in Materials Science and Engineering, 2015*, 1-5.

Hirjau, M., MD, Nicoara, A. C., MD, Hirjau, V., MD, PhD, & Lupuleasa, D., MD, PhD. (2011). Pelletization Techniques Used in Pharmaceutical Fields. *Practica Farmaceutică, 4*, 3-4.

Kitamura, T., & Komori, M. (1990). *Levitational Bearing Systems by Meissner Effect* (H. Reichl, Ed.). Berlin, Heidelberg: Springer Berlin Heidelberg.

Kittel, C. (2005). *Introduction to Solid State Physics $8^{th}$ edition*. New York: John Wiley & sons. Inc.

Mellekh, A., Zouaoui, M., Azzouz, F. B., Annabi, M., & Salem, M. B. (2006). Nano $Al_2O_3$ particle addition Effects on $YBaCu_2O_7$ superconducting properties. *Sol. Stat. Commun.*, 318-323

Li, G., Wang, M., & Yang, W. (2015). Enhanced Superconducting Properties in Infiltration Processed Y–Ba–Cu–O Single-grain Superconductor with Nano-sized Pinning Centers. *Journal of Alloys and Compounds, 649*, 559-563.

Miller, L., & Mullin, J. (2012). *Electronic Materials: From Silicon to Organics.*

Mitic, V. V., Paunovic, V., Pavlovic, V., & Zivkovic, L. (2011). Sintering Process Influence on Microstructure and Intergranular Impedance of Rare-Earth Modified BaTiO3- Ceramics. *Science of Sintering, 43*, 277-287.

Murakami, M. (1992). Processing of Bulk YBaCuO. *Superconductor Science and Technology, 5*(4), 185-203.

Prayoonphokkharat, P., Jiansirisomboon, S., & Watcharapasorn, A. (2013). Fabrication and properties of YBa2Cu3O7−x ceramics at different sintering temperatures. *Electronic Materials Letters, 9*(4), 413-416.

Schrieffer, J. (2007). *Handbook of High Temperature superconductor.* Springer

Sirisha K., V. R., Suresh, K., Vijayasree, K., Devanna, N., & Murthy, P. N. (2014). Recent Advances in Pelletization Techniques - A Review. *Int. J. Pharm. Sci. Rev. Res., 27*(1), 217-223.

Suzuki, M., & Suzuk, I. S. (2007, January 16). *Lecture Note on Solid State Physics Ginzburg-Landau Theory for Superconductivity.* Lecture presented at Ginzburg-Landau Theory for Superconductivity in Department of Physics, State University of New York at Binghamton, Binghamton, New York 13902-6000.

Terzieva S., Stoyanova A., Zalamova K., Mikli V., Angelov C., Kovachev V. Morphology of $Y_1Ba_2Cu_3O_z$ and $Y_{0.7}Ca_{0.3}Ba_2Cu_3O_z$ Bulk Samples Depending on Ca-substitution, J. Optoelec. Adv. Mat. 7 (2005) 477-480.

Valdes, L. (1954, February). Resistivity Measurements on Germanium for Transistors. *Proceedings Of The I-R-E,* 420-427.

Wu, M., Ashburn, J., Torng, C., Hor, P., Meng, R., Gao, L., Chu, C. (1987). Superconductivity at 93 K in a New Mixed-phase Y-Ba-Cu-O Compound System at Ambient Pressure. *Phys. Rev. Lett, 58*(9), 908-910.

## Calculation of Material Use

$$Y_2O_3 + 4BaCO_3 + 6CuO \longrightarrow t$$

Molar Mass $= (225.81) + 4(197.33) + 6(79.55)$

$= 1492.47 \text{ g/mol}$

To produce 50 g of $YBa_2Cu_3O_7$,

| $Y_2O_3$ | : | $x$ g | : | 1 mol | : | 225.81 g/mol |
| t | : | 50 g | : | 1 mol | : | 1492.47 g/mol |

$$\frac{x}{50} = \frac{1(225.81)}{1(1.492.47)}\frac{g}{mol}$$
$$x = (50)\times\frac{1(225.81)}{1(1.492.47)}\frac{g}{mol}$$
$$x = 7.55g$$

| $BaCO_3$ | : | $y$ g | : | 4 mol | : | 197.34 g/mol |
| t | : | 50 g | : | 1 mol | : | 1492.47 g/mol |

$$\frac{y}{50} = \frac{4(197.34)}{1(1.492.47)}\frac{g}{mol}$$
$$y = (50)\times\frac{1(197.34)}{1(1.492.47)}\frac{g}{mol}$$
$$y = 26.45 \text{ g}$$

| CuO | : | $z$ g | : | 2 mol | : | 79.55 g/mol |
| t | : | 50 g | : | 1 mol | : | 1492.47 g/mol |

$$\frac{z}{50} = \frac{2(79.55)}{1(1.492.47)}\frac{g}{mol}$$
$$z = (50)\times\frac{2(79.55)}{1(1.492.47)}\frac{g}{mol}$$
$$z = 16.0 \text{ g}$$

Therefore, the amount of $Y_2O_3$, $BaCO_3$ and CuO required to produce 50 g of $YBa_2Cu_3O_7$, are 7.55 g, 26.45 g and 16.0 g respectively.

APPENDIX B

**Lattice Parameter Calculation**

$$\frac{1}{d^2} = \frac{h^2}{a^2} + \frac{k^2}{b^2} + \frac{l^2}{c^2}$$

For YBCO + 0.00 wt% PbO

At (0 1 0) plane

$$\frac{1}{3.889^2} = \frac{1^2}{b^2}$$

$b = 3.889 \text{ Å}$

At (2 2 0) plane

$$\frac{1}{1.366^2} = \frac{2^2}{a^2} + \frac{2^2}{3.889^2}$$

$$\frac{4}{a^2} = 0.5359 - 0.2645$$

$$\frac{a^2}{4} = 3.6840$$

$a = 3.8387 \text{ Å}$

At (0 1 4) plane

$$\frac{1}{2.3305^2} = \frac{1^2}{3.889^2} + \frac{4^2}{c^2}$$

$$\frac{16}{c^2} = 0.1841 - 0.0661$$

$$\frac{c^2}{16} = 8.4746$$

$c = 11.644 \text{ Å}$

Therefore, the lattice parameter for non-added YBCO sample is

$a = 3.8387 \text{ Å}, b = 3.889 \text{ Å}$ and $c = 11.644 \text{ Å}$.

For YBCO + 0.01 wt% PbO

At (0 0 2) plane

$$\frac{1}{5.809^2} = \frac{2^2}{c^2}$$

$$c = 11.618 \text{ Å}$$

At (0 1 2) plane

$$\frac{1}{3.197^2} = \frac{1^2}{b^2} + \frac{2^2}{11.618^2}$$

$$\frac{1}{b^2} = 0.0978 - 0.0296$$

$$\frac{b^2}{1} = 14.6702$$

$$b = 3.8291 \text{ Å}$$

At (1 1 2) plane

$$\frac{1}{2.4656^2} = \frac{1^2}{a^2} + \frac{1^2}{3.8291^2} + \frac{2^2}{11.618^2}$$

$$\frac{1}{a^2} = 0.1645 - 0.0682 - 0.0296$$

$$a^2 = 14.9925$$

$$a = 3.8721 \text{ Å}$$

Therefore, the lattice parameter for non-added YBCO sample is

$a = 3.8721$ Å, $b = 3.8291$ Å and $c = 11.618$ Å.

For YBCO + 0.02 wt% PbO

At (0 2 0) plane
$$\frac{1}{1.9079^2} = \frac{2^2}{b^2}$$
$$b = 3.8158 \text{ Å}$$

At (0 0 3) plane
$$\frac{1}{3.873^2} = \frac{3^2}{c^2}$$
$$b = 11.619 \text{ Å}$$

At (1 0 3) plane
$$\frac{1}{2.7390^2} = \frac{1^2}{a^2} + \frac{3^2}{11.619^2}$$
$$\frac{1}{a^2} = 0.1333 - 0.0667$$
$$a^2 = 15.015$$
$$a = 3.8750$$

Therefore, the lattice parameter for non-added YBCO sample is
$$a = 3.8750 \text{ Å}, b = 3.8158 \text{ Å and } c = 11.619 \text{ Å}$$

For YBCO + 0.03 wt% PbO

At (2 0 0) plane
$$\frac{1}{1.9114^2} = \frac{2^2}{a^2}$$
$a = 3.8228\ \text{Å}$

At (0 2 0) plane
$$\frac{1}{1.9465^2} = \frac{2^2}{b^2}$$
$b = 3.8930\ \text{Å}$

At (0 0 3) plane
$$\frac{1}{3.893^2} = \frac{3^2}{c^2}$$
$c = 11.679\ \text{Å}$

Therefore, the lattice parameter for non-added YBCO sample is

$a = 3.8228\ \text{Å}, b = 3.8930\ \text{Å}$ and $c = 11.679\ \text{Å}$.

For YBCO + 0.04 wt% PbO

At (2 0 0) plane
$$\frac{1}{1.9082^2} = \frac{2^2}{a^2}$$
$$a = 3.8164 \text{ Å}$$

At (0 1 0) plane
$$\frac{1}{3.877^2} = \frac{1^2}{b^2}$$
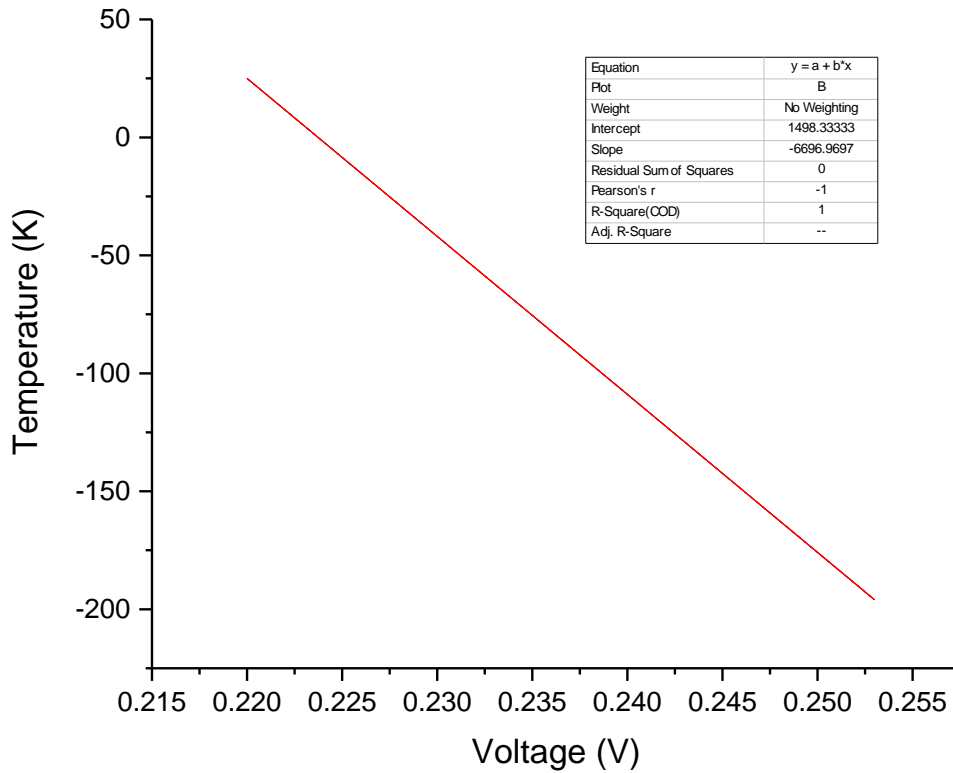$$b = 3.877 \text{ Å}$$

At (0 0 7) plane
$$\frac{1}{1.6654^2} = \frac{7}{c^2}$$
$$c = 11.658 \text{ Å}$$

Therefore, the lattice parameter for non-added YBCO sample is
$a = 3.8164$ Å, $b = 3.877$ Å and $c = 11.658$ Å.

**Calculation of critical temperature, T$_c$**



| Equation | y = a + b*x |
|---|---|
| Plot | B |
| Weight | No Weighting |
| Intercept | 1498.33333 |
| Slope | -6696.9697 |
| Residual Sum of Squares | 0 |
| Pearson's r | -1 |
| R-Square(COD) | 1 |
| Adj. R-Square | -- |

Using the function of the line $y = -6696.97x + 1498.33$, the corresponding recorded temperature of the thermocouple was calculated.

The resistance was calculated using the formula;

$V = IR$

$R = \dfrac{I}{V}$

The graph of resistance against temperature was then plotted as shown in Figure 4.11 to Figure 4.14